

DEPARTMENT OF ELECTRICAL AND COMPUTER ENGINEERING

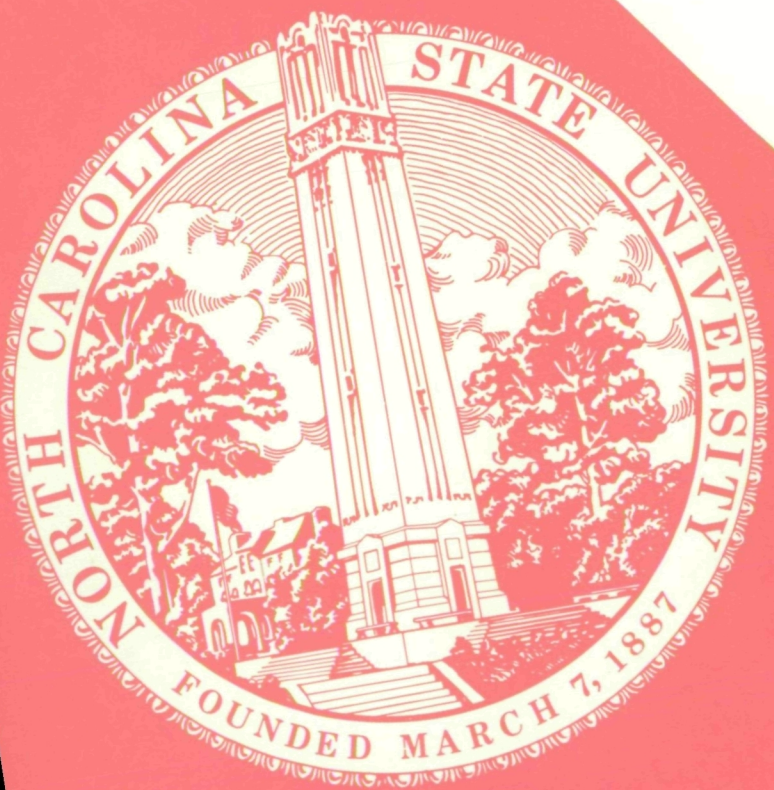
NSG-1588

IN-11649

N86-27516

(NASA-CR-177235) ON THE CONVERGENCE OF AN ITERATIVE FORMULATION OF THE ELECTROMAGNETIC SCATTERING FROM AN INFINITE GRATING OF THIN WIRES (North Carolina State Univ.) 99 P
HC A05/MF A01 CSCL 20N G3/32

Unclas
43246



SCHOOL OF ENGINEERING

ON THE CONVERGENCE OF AN ITERATIVE FORMULATION
OF THE ELECTROMAGNETIC SCATTERING
FROM AN INFINITE GRATING OF THIN WIRES

by

JERRY C. BRAND

DEPARTMENT OF ELECTRICAL AND COMPUTER ENGINEERING
NORTH CAROLINA STATE UNIVERSITY
Raleigh, North Carolina

May 1985

This research was supported by the National Aeronautics and Space Administration through grant NSG 1588.

ABSTRACT

Contraction theory is applied to an iterative formulation of electromagnetic scattering from periodic structures and a computational method for insuring convergence is developed. A short history of spectral (or k-space) formulation is presented with an emphasis on application to periodic surfaces. The mathematical background for formulating an iterative equation is covered using straightforward single variable examples including an extension to vector spaces. To insure a convergent solution of the iterative equation, a process called the contraction corrector method is developed. Convergence properties of previously presented iterative solutions to one-dimensional problems are examined utilizing contraction theory and the general conditions for achieving a convergent solution are explored. The contraction corrector method is then applied to several scattering problems including an infinite grating of thin wires with the solution data compared to previous works. Problems associated with extending the contraction corrector method to two-dimensional iterative formulations are outlined including the benefits of applying this process to difficult practical problems such as knitted mesh surfaces.

ACKNOWLEDGEMENTS

The author wishes to thank all the people who have helped him in the completion of his graduate work. In particular, he expresses deepest appreciation to his major advisor, Professor J. Frank Kauffman, who was first a friend and then a mentor in many situations. Special thanks are extended to the people in the RF Subsystems Section for the support they offered, and especially to Linda Snyder and Susan Sanders for their help in typing.

The author also wishes to express his thanks to his wife who gave so much support in the completion of this dissertation and for the final typing of the dissertation.

TABLE OF CONTENTS

iv

	Page
LIST OF TABLES	v
LIST OF FIGURES	vi
I. INTRODUCTION	1
II. REVIEW OF THE FUNDAMENTAL FORMULATION	4
III. MATHEMATICAL FORMULATION OF ITERATIVE EQUATIONS, CONTRACTIONS AND FIXED- POINT THEORY	12
IV. THE PERIODIC STRUCTURE: A CANONICAL CASE AND THE REGIONS OF SOLVABILITY	23
V. THE PROBLEM OF AN INFINITE GRATING OF THIN WIRES	48
VI. EXTENSION TO TWO-DIMENSIONAL PROBLEMS	61
VII. CONCLUSIONS	74
REFERENCES	76
APPENDIX A	79
APPENDIX B	86
APPENDIX C	90

LIST OF TABLES

v

	Page
Table 1. Example of a convergent iterative equation.	16
Table 2. Example of a non-convergent iterative equation with convergence achieved by applying the contraction corrector method.	19
Table 3. Example of a complex valued iterative equation and the use of a complex contraction corrector.	21
Table 4. Example of a two-variable contraction corrector method.	67

LIST OF FIGURES

Figure 1.	a) The planar periodic surface indicating electric current density \bar{J}_{mn} over the conducting portion and \bar{K}_{mn} over the aperture portion	
	b) Unit cell definition	8
Figure 2.	Example of convergent iterative equation $g(x)$	15
Figure 3.	Free-standing conducting strips with Floquet cell width a , aperture size b and conductivity σ	32
Figure 4.	Convergence of the aperture \bar{E} field for $a=1.4\lambda$, $b=0.6\lambda$, $\theta=0^\circ$ case using equation (40)	35
Figure 5.	Convergence of the aperture \bar{E} field for $a=1.4\lambda$, $b=0.6\lambda$, $\theta=0^\circ$ case using equation (40) with the correction of equation (53) applied, from Tsao and Mittra [9]	36
Figure 6.	Convergence of the aperture \bar{E} field for $a=1.4\lambda$, $b=0.6\lambda$, $\theta=0^\circ$ case using equation (42). This is the contraction corrector method	38
Figure 7.	Contraction factor for a cell width of 1.4λ , incidence angle $\theta=0^\circ$ with H-wave polarization and $\phi=0^\circ$	39

Figure 8.	Contraction factor for a strip width of 0.6λ , incidence angle $\theta=0^\circ$ with H-wave polarization and $\phi=0^\circ$	40
Figure 9.	Contraction factor for a strip width of 0.1λ , incidence angle of $\theta=0^\circ$ with H-wave polarization and $\phi=0^\circ$	42
Figure 10.	Convergence survey using contraction criteria for $0^\circ < \theta < 90^\circ$, $\phi=0^\circ$, $a=0.9\lambda$, and $b=0.4\lambda$	43
Figure 11.	a) Non-convergent results of the variational corrected iterative equation for $\theta=70^\circ$	45
	b) Non-convergent results for the basic iterative equation with $\theta=70^\circ$	46
Figure 12.	Convergent results obtained from the contraction corrector method of equation (30) with $\phi=0^\circ$, $\theta=70^\circ$, $a=1.4\lambda$ and $b=0.6\lambda$	47
Figure 13.	Planar grid of thin conducting wires.	49
Figure 14.	Convergence properties of the variational correction scheme using both $\bar{E}^{(n)}$ and the Dirac delta function as the test function with $\theta=\phi=0^\circ$, $a=0.25\lambda$ and $b=0.247\lambda$	50
Figure 15.	Definition of reflection coefficients as described in [22].	53

	Page
Figure 16. Comparison of results obtained from Wait [2] and equation (30) for various cell widths with $\phi=0^0$, $0<\theta<90^0$, and $\sigma=\infty S$.	55
Figure 17. Reflection coefficient as defined in Figure 15 for $\phi=90^0$, $0^0<\theta<90^0$, $a=0.247\lambda$ and $\sigma=\infty S$.	56
Figure 18. Several cases of finite conductivity with $\theta=0^0$, $0^0<\theta<90^0$, $a=0.25\lambda$ and $b=0.247\lambda$.	58
Figure 19. Illustration of converged accuracy for various number of terms with $a=0.25\lambda$, $b=0.247\lambda$, $\theta=\phi=0^0$ and $\sigma=\infty S$.	60
Figure 20. Actual mesh surface.	69
Figure 21. Floquet cells outlined on the actual mesh surface.	71
Figure 22. Single mesh path of the actual mesh surface.	72
Figure 23. Grid representation of the segmented single mesh path.	73

I. INTRODUCTION

The electromagnetic scattering properties of periodic structures have been of interest to engineers and scientists for many years and various methods for solving the scattering problem have been presented [1] - [8] . These methods include solutions generated from static approximations, averaged boundary conditions, the method of moments, physical optics, the geometrical theory of diffraction, and a combination of these techniques. However, certain frequency regions or certain geometrical configurations (or both) cause grave difficulties which cannot be overcome by the methods mentioned above.

Tsao and Mittra [9] presented a novel iterative technique based on earlier spectral approaches which can be traced to original work performed by Bojarski [10] . This technique, called the spectral-iteration approach, extended the scattering solution capability to regions previously untouched by other methods. In particular, Tsao and Mittra [9] examined the scattering from periodic structures and their applications to frequency selective surfaces. The present author's area of interest is the problem of determining the reflection properties of mesh surfaces [11] . Mesh surfaces are used in many applications, but the most current application is for conducting reflectors on space-borne antennas. The mesh surface is a complex

periodic structure whose reflecting properties are not readily analyzed by the methods mentioned above. For instance, an attempt to solve the mesh problem by the method of moments would require a special set of basis functions as well as an enormous amount of computer memory. Analysis of the mesh surface by the spectral-iteration technique would be of great value since the method is essentially independent of geometry, i.e., does not require explicit knowledge of appropriate basis functions and does not require extreme amounts of computer storage. However, the basic iterative scheme suffers from convergence problems that are associated with most iterative formulations [12]. This work treats basic iterative techniques, presents a background on the convergence problems associated with iterative techniques, details the formulation of a corrective scheme to insure convergence of the iterative technique, and applies a version of the corrective scheme to the specialized problem of a parallel wire grating.

Current techniques for solving complex scattering problems are limited by the difficulties outlined above. The technique described herein provides a basis for the further development of solutions to complex problems. Additionally, the solution methodology provides a useful concept which may be applied to problems outside the realm of electromagnetic scattering.

Portions of the background material presented below follow directly from the referenced works and credits are listed for these. The notation used herein is self contained with attempts to follow the references as closely as possible to maintain a common base, but allowing for differences to insure clarity of the equations. This is included for consistency, completeness, and continuity. The reader is advised to consult the references for greater detail.

II. REVIEW OF THE FUNDAMENTAL FORMULATION

Bojarski [10] considered that field quantity $\Psi(x)$ and a source density $w(x)$ were governed by the differential equation

$$L_{\Psi}\Psi(x) = -L_w w(x) \quad (1)$$

where the form of the operators for an n-dimensional problem are

$$L_{\Psi} = \sum_{i=0}^m a_i \left(\frac{\partial^i}{\partial x_p^i} \right) \quad ; \quad p=1,2,\dots,n \quad (2)$$

and

$$L_w = \sum_{i=0}^m b_i \left(\frac{\partial^i}{\partial x_p^i} \right) \quad ; \quad p=1,2,\dots,n \quad (3)$$

subject to the constitutive equation

$$w(x) = q(x) \cdot \Psi(x) \quad (4)$$

The generalized integral representation of equation (1) is given by

$$\Psi(x) = \int g(x, x') \cdot w(x') d^n x' + \Psi_{inc}(x) \quad (5)$$

where $g(x, x')$ is the appropriate Green function satisfying equation (1) with $w(x)$ replaced by $\delta(x)$, the Dirac delta function and Ψ_{inc} being the externally applied field.

Equation (5) is the basic equation which is to be solved by application of a transform technique.

The Fourier transform of a function $f(x)$ is given as

$$\tilde{f}(k) = \int_{-\infty}^{\infty} f(x) e^{jk \cdot x} dx \quad (6)$$

and the transform pairs formed are noted as $\tilde{f}(k) \leftrightarrow f(x)$.

Thus, by taking the Fourier transform of equations (1), (2), and (3), the k-space formulation of the problem becomes

$$\tilde{L}_{\psi}(k) \tilde{\Psi}(k) = \tilde{L}_w(k) \tilde{w}(k) \quad (7)$$

$$\tilde{L}_{\psi}(k) = \sum_{i=0}^m a_i (jk)^i \quad (8)$$

$$\tilde{L}_w(k) = \sum_{i=0}^m b_i (jk)^i \quad (9)$$

where j is the usual imaginary counter-clockwise rotation operator. The integral equation (5) then becomes

$$\tilde{\Psi}(k) = \tilde{g}(k) \tilde{w}(k) + \tilde{\Psi}_{inc}(k) \quad (10)$$

still subject to the conditions of equation (4). This approach yields two algebraic equations which may usually be solved with much less effort than equation (5). With

this thought in mind, we now examine the application of this procedure to the problem of electromagnetic scattering from a periodic structure.

The electric field \bar{E} generated from an equivalent magnetic source \bar{K} can be represented by

$$\bar{E}(x,y,z) = \frac{-1}{\epsilon} \nabla \times \bar{F}(x,y,z) \quad (11)$$

where \bar{F} is the associated electric vector potential of the source and ϵ is the permittivity of the medium [13]. The relationship between \bar{F} and \bar{K} is established with the use of the position vector \bar{r} and the free space Green function

$$\bar{G} = \frac{e^{-j(\hat{k} \cdot \hat{r})}}{4\pi |\bar{r}|} \bar{I} \quad (12)$$

by

$$\bar{F}(\bar{r}) = \int \bar{G}(\bar{r}, \bar{r}') \cdot \bar{K}(\bar{r}') d\bar{r}' \quad (13)$$

where \hat{k} and \hat{r} are the respective unit vectors of the problem. From this, the magnetic field intensity \bar{H} can be derived from Maxwell's equations and is given by

$$\bar{H}(x,y,z) = -j\omega\epsilon \bar{F}(x,y,z) + \frac{\nabla \cdot \bar{F}(x,y,z)}{j\omega\mu} \quad (14)$$

where μ is the permeability of the medium. For the xy planar set of magnetic currents shown in Figure 1, $F_z=0$ is

obtained from equation (13) since $z=0$ and \vec{G} is then a function of x and y only. Allowing the medium to be that of free space, i.e. $\epsilon = \epsilon_0$ and $\mu = \mu_0$, and since $F_z = 0$, equation (14) is expanded in Cartesian coordinates x and y to yield for $z=0$

$$\begin{aligned} \vec{H}_s(x,y) = \frac{1}{j\omega\mu_0} \left[\left(k_0^2 \vec{F}_x + \frac{\partial^2 \vec{F}_y}{\partial x \partial y} + \frac{\partial^2 \vec{F}_x}{\partial x^2} \right) \hat{x} \right. \\ \left. + \left(k_0^2 \vec{F}_y + \frac{\partial^2 \vec{F}_x}{\partial x \partial y} + \frac{\partial^2 \vec{F}_y}{\partial y^2} \right) \hat{y} \right] \end{aligned} \quad (15)$$

where $k_0 = \omega \sqrt{\mu_0 \epsilon_0}$ is the propagation constant. The quantity given by equation (15) is a general representation for the scattered magnetic field intensity generated from a planar source of magnetic current in the xy plane.

Consider the planar periodic surface shown in Figure 1 to be the source distribution for the magnetic field of equation (15). Upon substituting equation (13) into equation (15) and taking the Fourier transform of equation (15) we obtain

$$\vec{H}_s(\alpha, \beta) = \frac{1}{j\omega\mu_0} \sum_{mn} \begin{bmatrix} k_0^2 - \alpha_{mn}^2 & \alpha_{mn} \beta_{mn} \\ -\alpha_{mn} \beta_{mn} & k_0^2 - \beta_{mn}^2 \end{bmatrix} \quad (16)$$

$$\vec{G}(\alpha_{mn}, \beta_{mn}) \vec{K}(\alpha_{mn}, \beta_{mn}) e^{j(\alpha_{mn}x + \beta_{mn}y)}$$

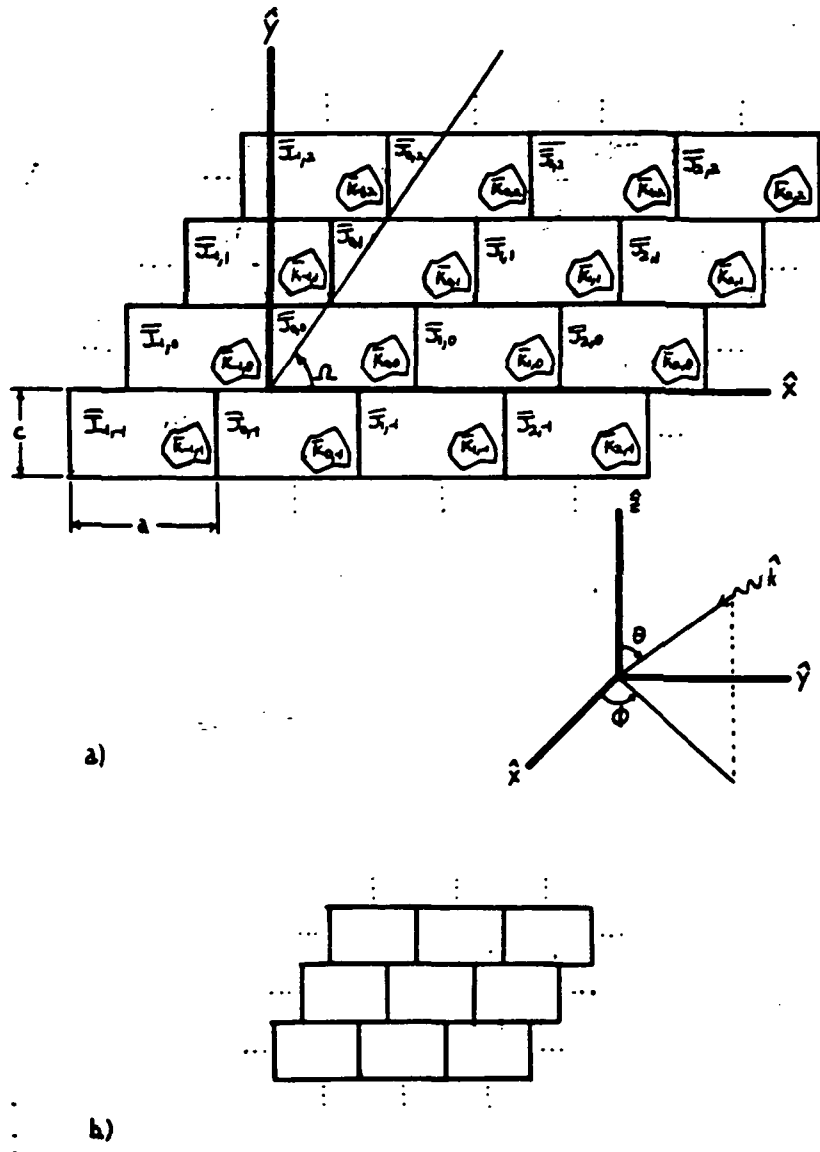


Figure 1. a.) The planar periodic surface indicating electric current density \vec{J}_{mn} over the aperture portion.
b.) Unit cell definition.

for the transformed magnetic field where

$$\alpha_{mn} = \frac{2\pi m}{a} - k_0 \sin\theta \cos\phi \quad (17)$$

$$\beta_{mn} = \frac{2\pi n}{c} - \frac{2\pi m}{a} \cot\Omega - k_0 \sin\theta \sin\phi \quad (18)$$

are the Floquet modes [14] and

$$\tilde{G}(\alpha_{mn}, \beta_{mn}) = \frac{-j}{2(k_0^2 - \alpha_{mn}^2 - \beta_{mn}^2)^{1/2}} \quad \bar{I} \quad (19)$$

is the Fourier transform of the dyadic Green function [9]. The discrete nature of equation (16) results from taking the Fourier transform of a periodic function [15]. The final step in completing the process of obtaining a useable form of the magnetic field intensity in the aperture is accomplished by taking the inverse Fourier transform of equation (16), noting $\bar{K} = \bar{E}_a X \hat{z}$, using the equivalence theorem and applying the appropriate boundary conditions on $\bar{H}^s(x, y)$ at $z=0$ [9]. This leads to

$$\bar{H}_{\text{tinc}}(x, y) = \frac{-2}{j \omega \mu_0} \sum_{mn} \begin{bmatrix} \alpha_{mn} \beta_{mn} & k_0^2 - \alpha_{mn}^2 \\ -k_0^2 + \beta_{mn}^2 & -\alpha_{mn} \beta_{mn} \end{bmatrix} \quad (20)$$

$$\bar{G}(\alpha_{mn}, \beta_{mn}) \tilde{E}_a^+(\alpha_{mn}, \beta_{mn}) e^{j(\alpha_{mn} x + \beta_{mn} y)}$$

where $\tilde{\mathbf{E}}_a^+(\alpha_{mn}, \beta_{mn})$ is the transformed electric field in the aperture and $\tilde{\mathbf{H}}_{\text{tinc}}(x,y)$ is the incident tangential magnetic field. The inverse of equation (20) is obtained by extending the operations over the entire unit cell. The extended operator is necessary to insure the operations indicated by equation (20) are in the domain of the solution. That is, the boundary conditions of the problem are satisfied. This extension is accomplished by including the electric current density over the conducting portion of the unit cell. The electric current density is included by introducing the truncation operator and the complement truncation operator defined as

$$\begin{aligned} T(f(\bar{r})) &= 0 && \text{for } \bar{r} \text{ on the conductor} \\ T(f(\bar{r})) &= f(\bar{r}) && \text{for } \bar{r} \text{ in the aperture} \end{aligned} \quad (21)$$

and

$$\begin{aligned} T_c(f(\bar{r})) &= 0 && \text{for } \bar{r} \text{ in the aperture} \\ T_c(f(\bar{r})) &= f(\bar{r}) && \text{for } \bar{r} \text{ on the conductor} \end{aligned} \quad (22)$$

This allows equation (20) to be extended over the unit cell as

$$T_c \left(\bar{J}(x,y) \right) = \bar{H}_{\text{tinc}}(x,y) + \frac{2}{j\omega\mu_0} \sum_{mn} \begin{bmatrix} \alpha_{mn}\beta_{mn} & k_0^2 - \alpha_{mn}^2 \\ -k_0^2 + \beta_{mn}^2 & -\alpha_{mn}\beta_{mn} \end{bmatrix} \quad (23)$$

$$\tilde{G}(\alpha_{mn}, \beta_{mn}) \tilde{E}_a^+(\alpha_{mn}, \beta_{mn}) e^{j(\alpha_{mn}x + \beta_{mn}y)}$$

with $\bar{J}(x,y)$ representing the electric current density on the conductor. Equation (23) is a form which can readily lend itself to solution by iterative techniques.

III. MATHEMATICAL FORMULATION OF ITERATIVE EQUATIONS CONTRACTIONS AND FIXED-POINT THEORY

The use of iterative equations to solve mathematical problems has been around for many centuries dating back to B.C. 600 when this technique was used to solve problems such as determining the square root of three. Beginning with this early exploration of iterative techniques came the plights of correct problem formulation and convergence of the solution. Later methods, such as Newton's method of solution, alleviated such problems but often forced other constraints on the problem. One such constraint is that the initial solution estimate needs to be in a region reasonably close to the desired solution. Tsao and Mittra [9] used this spirit of a priori knowledge in the form of a variational correction to remain near the solution point in their problem formulation. However, as will be demonstrated later, the cases presented in their work did not require such a correction and, indeed, they even noted where the iteration method failed even using such a correction.

The idea of using the iterative scheme to solve general scattering problems leads one to seek a way of determining the criteria for convergence and a way of generating a convergent iterative formulation. Fixed-point theory and contractor theory [16, 17] are applied to formulate a con-

vergent iterative solution to the scattered fields derived in Chapter II.

The general idea of fixed-point theory revolves around finding the solution to an equation such as

$$f(x) = y = x^2 - 6x + 5 = (x-5)(x-1) = 0 \quad (24)$$

This is accomplished by forming an iteration function as

$$x_{n+1} = g(x_n) \quad (25)$$

and finding the intersection $y=g(x_n)$ and $y=x_n$ which yields the fixed-point and solution to equation (24). This is accomplished by starting with an initial guess x_0 , substituting into equation (25) to generate x_1 , and continuing this process until $x_{n+1}=x_n+e$ where e is the allowed error. At this time $x=x_{n+1}$ is the approximate solution to equation (25). The conditions for a convergent solution are in general:

a.) on a closed interval I , $g(x)$ maps I into itself

b.) $g(x)$ is continuous on I

and c.) $g(x)$ is differentiable on I and $\left| \frac{dg(x)}{dx} \right| < 1$

Thus the following theorem may be stated

Theorem 1. Let $g(x)$ satisfy conditions a.), b.), and c.). Then $g(x)$ has exactly one fixed point x^* in I and starting with any x_0 in I , the sequence x_0, x_1, \dots, x_n generated by equation (25) converges to x^* .

The process outlined by the above theorem is illustrated in Figure 2. The fixed-point x^* is often said to be a point of attraction for $g(x)$. x_{n+1} is also said to contract to x^* .

To illustrate the use of this theory, one root of equation (24) will be determined. Let

$$x_{n+1} = g(x_n) = \frac{x_n^2 + 5}{6} \quad (26)$$

and find

$$\frac{d}{dx} g(x) = \frac{x}{3} \quad (27)$$

then, the interval I is defined as $x \in I$ and $I \subset [-3, 3]$. Note that the known root $x=1$ is in this interval and $\left. \frac{d}{dx} g(x) \right|_{x=1} = 1/3$. We then expect that the iteration function will converge to the fixed-point $x^*=1$ which is the correct solution. The iterative process is contained in Table 1. The question then arises, what happens when the sequence will not converge?

To generate an iterative equation that will converge we must meet the conditions listed in Theorem 1 above. As an example, let us examine the roots of

$$f(x) = x^2 - x - 6 = (x+2)(x-3) \quad (28)$$

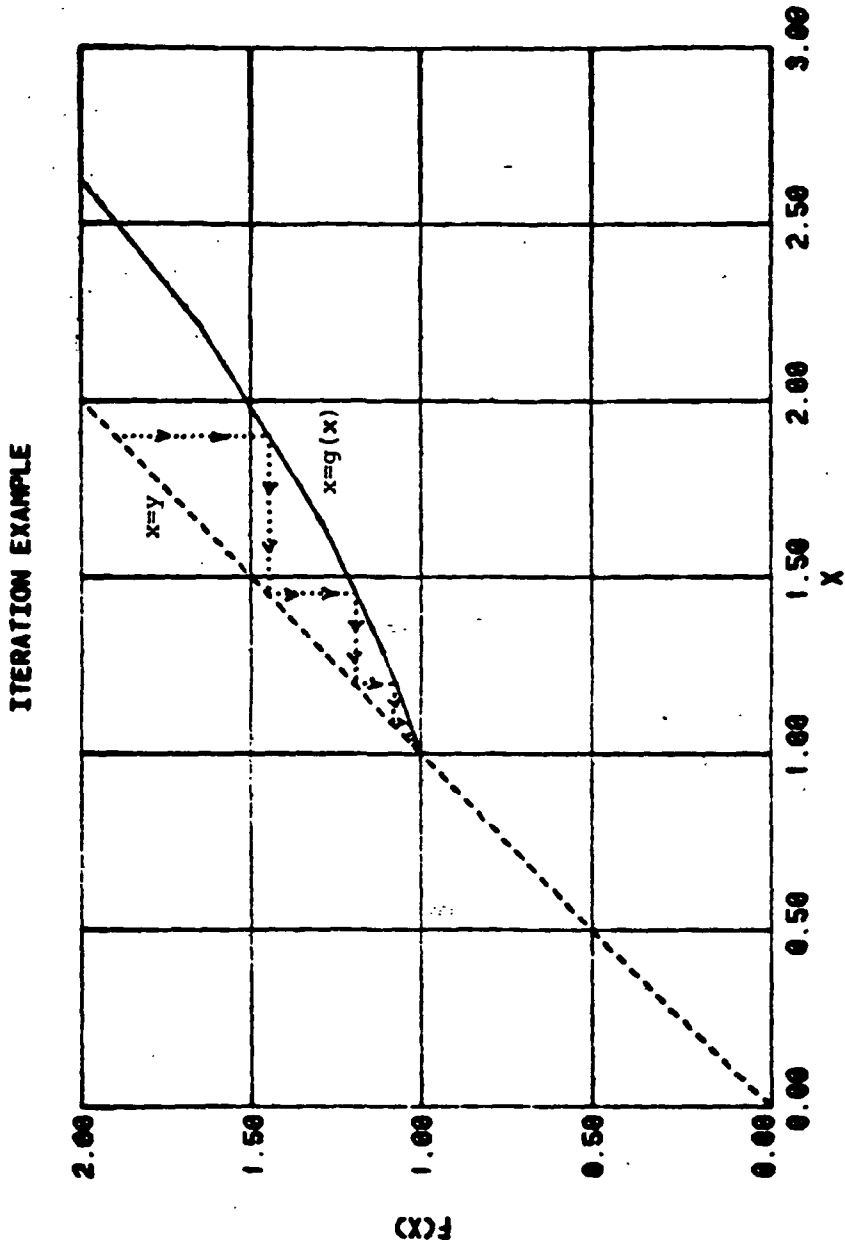


Figure 2. Example of convergent iterative equation $g(x)$.

$$f(x) = x^2 - 6x + 5 = 0$$

$$g(x) = x = \frac{x^2 + 5}{6}$$

	$g(x)$
x_0	2.0
x_1	1.5
x_2	1.208
x_3	1.077
x_4	-1.026
x_5	1.009
x_6	1.003
	⋮
	⋮
x_{n-1}	
$x^* = x_n$	1.000

Table 1. Example of a convergent iterative equation

which can be seen to be -2 and 3. By forming the iterative equation

$$g(x_n) = x_{n+1} = x_n^2 - 6 \quad (29)$$

and noting

$$\left| \frac{d}{dx} g(x) \right| = |2x|_{x=-2,3} > 1 \quad (30)$$

we see that the iterative equation will not converge. However, by properly forming a new iterative equation $G(x)$ that has $\left| \frac{d}{dx} G(x) \right|_{x=-2} < 1$, or $\left| \frac{d}{dx} G(x) \right|_{x=3} < 1$, the roots may be obtained. Although manipulation of equation (29) could yield a suitable $G(x)$ [12] we seek a $G(x)$ that can be formed by a method known as relaxation. The relaxation process generally uses a portion of the n^{th} iteration along with a portion of the iterated n^{th} (i.e. $n+1$) iteration to "relax" the process. The form of the relaxed iterative equation is

$$G(x_n) = Rx_n + (1-R)g(x_n) \quad (31)$$

where R is called the relaxation constant. The condition

$$\left. \frac{d}{dx} G(x) \right|_{x=x_n} = 0 \quad (32)$$

may be used to determine an optimum R such that convergence

of $G(x)$ is assured. Performing the operation of equation (32) on equation (31) yields

$$\left. \frac{d}{dx} G(x) \right|_{x=x_n} = R + (1-R) \left. \frac{d}{dx} g(x) \right|_{x=x_n} = 0 \quad (33)$$

and solving for the linear correction R

$$R = \frac{g'(x)}{g'(x) - 1} \quad (34)$$

where $g'(x) = \left. \frac{d}{dx} g(x) \right|_{x=x_n}$. This process of finding the optimum R is called the contraction corrector (a name to be explained later in this section) and is used to iteratively solve for the root $x=3$. This is illustrated in Table 2. Equivalence between the contraction corrector and Newton's method can be shown and is illustrated in Appendix C. Note that $g(x_n)$ would not converge by itself and thus $G(x_n)$ is necessary for a correct solution to be obtained. As a further note on the iterative process, the conditions that $g(x)$ maps I into itself is not trivial. For instance, note that

$$f(x) = x^2 + 2 = 0 \quad (35)$$

will not yield a solution from an iterative process unless x is allowed to be complex and $g(x)$ or $G(x)$ maps into the complex plane. The iterative equation $G(x)$ may even require a complex relaxation or complex contraction correction constant and precautions governing complex algebra

$$g(x_n) = x_{n+1} = x_n^2 - 6$$

$$x_{n+1} = G(x_n) = Rx_n + (1-R)g(x_n) = Rx_n + (1-R)(x_n^2 - 6)$$

$$R = \frac{2x_n}{2x_n - 1}$$

n	x_n	R_n	$g(x_n)$	$G(x_n)$
0	1.0	2.0	-5.0	7.0
1	7.0	1.07	43.0	4.24
2	4.24	1.13	11.98	3.23
3	3.23	1.18	4.43	3.01
4	3.01	1.2	3.06	3.0

n	x_n	$g(x_n)$
1	3.0001	3.0006
2	3.0006	3.0036
3	3.0036	3.0216
4	3.0216	3.130
5	3.130	3.798
6	3.798	8.424

Table 2. Example of a non-convergent iterative equation with convergence achieved by applying the contraction correction method.

and operations must be observed. In particular, the analytic nature of $f(x)$, $g(x)$, and $G(x)$ in the interval I should meet the requirements of Theorem 1. An illustration of the nature of these problems is given in Table 3. In two cases, a real x_0 never maps x_n into the complex plane and, as such, never yields a solution. Even applying the contraction corrector method with a real x_0 does not give a solution. Only the one case using a complex x_0 and the contraction corrector method converges. This follows from the conditions of Theorem 1. Since problems have been observed in the simple problems above, a proper choice of action is to pursue the corrective method in a more general sense.

Stakgold [18] has formed a very sound collection of theorems and definitions on the idea of metric spaces and their transformations, and the following material is condensed from his book with the advice that the reader consult his work for proofs and greater detail.

Definition 1. A transformation L of a metric space x into itself is Lipschitz continuous if there exists a ρ , independent of u and v , such that

$$d(Lu, Lv) \leq \rho d(u, v) \text{ for all } u, v \in x$$

where $d(\xi, \zeta)$ is a proper metric in x . When the definition above holds for some fixed $|\rho| < 1$, the operation of L is called a contraction on X .

$$f(x) = x^2 - x + 2 = 0$$

$$g(x_n) = x_n^2 + 2$$

$$g'(x_n) = 2x_n$$

$$\beta_n = \frac{g'(x_n)}{g'(x_n) - 1}$$

$$G(x_n) = \beta_n x_n + (1 - \beta_n) g(x_n)$$

n	x_n	$g(x_n)$
0	1.00	3.00
1	3.00	11.00
2	11.00	123.00
-	-	diverges

n	x_n	$g(x_n)$	$g'(x_n)$	β_n	$G(x_n)$
0	2.00	6.00	4.00	1.33	0.67
1	0.67	2.44	1.33	4.00	-4.67
2	-4.67	23.78	-9.33	0.90	-1.91
3	-1.91	5.66	-3.83	0.79	-0.34
4	-0.34	2.12	-0.69	0.41	1.11
5	1.11	3.24	2.23	1.81	-0.62
6	-	-	-	-	-

n	x_n	$g(x_n)$	β_n	$G(x_n)$
0	4.24 + j4.24	1.88 + j35.95	1.06 - j0.07	2.18 + j2.34
1	2.18 + j2.34	1.81 + j10.24	1.09 - j0.13	1.13 + j1.45
2	1.13 + j1.45	1.20 + j3.29	1.13 - j0.28	0.64 + j1.25
3	0.64 + j1.25	0.85 + j1.59	1.05 - j0.40	0.50 + j1.31

$$x^* = 0.5 + j1.32$$

Table 3. Example of a complex valued iterative equation and the use of a complex contraction corrector.

Theorem 2. Let the operator L be a contraction on a complete metric space X . Then, $u=Lu$ has one and only one solution in X which may be obtained from any initial starting point u_0 in X . Thus, $u_n \rightarrow u^*$ (the fixed-point) as $n \rightarrow \infty$ and u^* exists and is unique in X .

Note that u may have multiple components, i.e., $u=u(z_1, z_2, \dots, z_n)$ where z_i are complex coordinates. ρ as given by definition 1 is the description of the measure of a general derivative of an operator. Thus, the process used in the single variable examples earlier may be extended to higher dimensional spaces with more general operators. This theorem allows that the relaxed corrective iterative process outlined earlier is indeed a contraction, hence the name contraction corrector. This nomenclature is used to differentiate this scheme from other corrective schemes applied to iterative processes. The use of this definition and theorem as applicable to the spectral-iteration approach of equation (23) is detailed in the following section.

IV. THE PERIODIC STRUCTURE: A
CANONICAL CASE AND THE REGIONS OF SOLVABILITY

The total electric field for the structure shown in Figure 1 may be expressed in terms of the incident and scattered fields as [9]

$$\left(\begin{array}{c} E_x \\ E_y \end{array} \right) = \left\{ \begin{array}{l} \left(\begin{array}{c} E_{x,inc} \\ E_{y,inc} \end{array} \right) + \sum_{mn} \begin{bmatrix} \alpha_{mn} \beta_{mn} & k_0^2 - \alpha_{mn}^2 \\ -k_0^2 + \beta_{mn}^2 & -\alpha_{mn} \beta_{mn} \end{bmatrix} \tilde{G}(\alpha_{mn}, \beta_{mn}) \\ \left(\begin{array}{c} \tilde{E}_{ax, mn}^+ \\ \tilde{E}_{ay, mn}^+ \end{array} \right) e^{j(\alpha_{mn}x + \beta_{mn}y)} e^{k_{z, mn} z} \quad \text{for } z > 0 \\ \sum_{mn} \begin{bmatrix} \alpha_{mn} \beta_{mn} & k_0^2 - \alpha_{mn}^2 \\ -k_0^2 + \beta_{mn}^2 & -\alpha_{mn} \beta_{mn} \end{bmatrix} \tilde{G}(\alpha_{mn}, \beta_{mn}) \\ \left(\begin{array}{c} \tilde{E}_{ax, mn}^- \\ \tilde{E}_{ay, mn}^- \end{array} \right) e^{j(\alpha_{mn}x + \beta_{mn}y)} e^{-k_{z, mn} z} \quad \text{for } z < 0 \end{array} \right. \quad (36)$$

where

$$k_{z, mn} = \left\{ \begin{array}{ll} -j(k_0^2 - \alpha_{mn}^2 - \beta_{mn}^2)^{\frac{1}{2}} & \text{for } k_0^2 > \alpha_{mn}^2 + \beta_{mn}^2 \\ -(\alpha_{mn}^2 + \beta_{mn}^2 - k_0^2)^{\frac{1}{2}} & \text{for } k_0^2 < \alpha_{mn}^2 + \beta_{mn}^2 \end{array} \right. \quad (37)$$

and \tilde{E}_a^+ and \tilde{E}_a^- represent the transformed electric field and are respectively the reflection and transmission coefficients of the Floquet modes. Deriving \bar{H} from equation (36) and by enforcing the boundary conditions on the tangential magnetic fields across the cell at $z=0$, equation (23) is generated again. This exercise is presented to complete the field description and to illustrate the relationship between the aperture fields and the reflection and transmission coefficients as the coefficients will be of interest later in the section. Equation (23) is the beginning point to cast the problem in an iterative form.

The summation in equation (23) represents a discrete Fourier series (DFS) for an infinite duration (i.e., periodic) sequence [19]. This representation allows for direct transformation between the (x,y,z) domain and the (k_x, k_y, k_z) domain. Since the functions are represented by sequences with complex exponentials having a periodicity of $2\pi/m$ and $2\pi/n$, one period of the aperture distributions, that is one cell of the structure, can be used to completely specify the transform. The use of one period to represent a periodic function in this manner is known as the discrete Fourier transform (DFT). It is important to note that the transformation mentioned above is exact and this infers that no aliasing will occur when the DFT is performed. Aliasing can occur when a non-periodic function is truncated and

and transformed with a DFT. Since information about the original function is lost in the truncation, performing the inverse transform can never return the original function. However, when using exactly one period of the periodic function, the original function can be reconstructed when the DFT and inverse DFT are performed. The most common form of DFT algorithm is the fast Fourier transform (FFT) in which special properties of the DFT are exploited to decrease the computation time of the transform. Throughout this section, the DFT and its inverse are represented by F and F^{-1} respectively. Implicit functional dependence is also used to present a "cleaner" form of the equations.

With the above thoughts in mind, we may solve equation (23) in terms of \bar{E}_t as:

$$\bar{E}_t = F^{-1} \left[\bar{G}^{-1} \cdot F \left\{ \frac{j\omega\mu_0}{2} \left[T_c(\bar{J}) - \bar{H}_{tinc} \right] \right\} \right] \quad (38)$$

and, for clarity write equation (23) as:

$$T_c(\bar{J}) = T_c \left[\bar{H}_{tinc} + \frac{2}{j\omega\mu_0} F^{-1} \left\{ \bar{G} \cdot F \left[T(\bar{E}_t) \right] \right\} \right] \quad (39)$$

Note that the subscript indicating aperture field has been removed from equations (38) and (39) since the truncation operator is included and the tangential field \bar{E}_t over the entire cell is used. Solving for \bar{E}_t in equations (38) with

$T_c(\bar{J})$ substituted from equation (39) yields:

$$\bar{E}_t^{(n+1)} = F^{-1} \left[\frac{\bar{G}}{G}^{-1} \cdot F \left\{ \frac{j\omega\mu_0}{2} \left[T_c \left(\bar{H}_{tinc} + \frac{2}{j\omega\mu_0} F^{-1} \left\{ \frac{\bar{G}}{G} \cdot F \left[T \left(\bar{E}_t^{(n)} \right) \right] \right\} - \bar{H}_{tinc} \right] \right\} \right] \right] \quad (40)$$

This is the form of iterative equation given by Tsao and Mittra [9] and is the basic equation to which a scheme called the contraction corrector will be applied. The contraction factor must be less than 1.0 to have a convergent solution [18] and the contraction corrector scheme will allow this condition to be met.

The iterative equation for one-dimension (E_x or E_y) will converge if the conditions for a contraction given by Stakgold [18] are met. The proper metric for the space X and the operators in equation (40) is:

$$d(u,v) = \left[\left| \xi_1 - \zeta_1 \right|^2 + \left| \xi_2 - \zeta_2 \right|^2 + \dots + \left| \xi_n - \zeta_n \right|^2 \right]^{\frac{1}{2}} \quad (41)$$

where $u = (\xi_1, \xi_2, \dots, \xi_n)$ and $v = (\zeta_1, \zeta_2, \dots, \zeta_n)$ are the vectors in X and ξ, ζ represent the components of each vector. The u and v used in the metric $d(u,v)$ may be any u, v in X since the contraction must hold for all u, v in X . One logical choice for u and v is $\bar{E}^{(n)}$ and $\bar{E}^{(n+1)}$. This choice would allow the contraction process to be observed and

would give the relative error between each iteration. This also allows the regions of convergence to be determined. That is, for decreasing error, the solution is converging and for increasing error diverging. Since we are interested in the contraction to a fixed-point, a wiser choice for u and v is $\bar{E}^{(n)}$ and $(\bar{E}^{(n)} + e)$ where e is some small complex number. Thus, at each component of $\bar{E}^{(n)}$ we essentially have the ability to determine the general derivative of the operator at each element. The contraction corrector is a vector $\bar{R}^{(n)}$ with one element for each component of $\bar{E}^{(n)}$. The form of $\bar{R}^{(n)}$ is exactly that of equation (31) for a one-variable problem extended to an N component one-dimensional problem. This powerful concept allows the regions of convergence to be determined and allows the formulation of a convergent solution as

$$\bar{E}^{(n+1)} = \bar{R}^{(n)} \cdot \bar{E}^{(n)} + (\bar{I} - \bar{R}^{(n)}) \cdot L \bar{E}^{(n)} \quad (42)$$

with L being the operator defined by equation (40). Uniqueness of the solution is guaranteed since the problem was formulated from Maxwell's equations via a vector magnetic potential and the appropriate boundary conditions were applied. Note that this representation is for a one-dimensional scattering problem. Additional conditions are necessary for the general solution of two-dimensional problems [12]. These conditions and other considerations for two-

dimensional problems are discussed in Section VI.

The contraction corrector $\bar{R} = \{R_1, R_2, \dots, R_n\}$ must be determined in a general operator sense to behave as R in equation (34). This implies that closer examination of Definition 1 is warranted. The determination of an operator derivative must be formulated in terms of a contraction. The derivative must be expressed in an analytical form that allows the contraction to be determined numerically for each R_i of \bar{R} . Thus, equation (42) will guarantee a convergent solution when \bar{R} is properly determined. The contraction is related to the continuity of the operator (transformation) L through Definition 1 as:

$$d(Lu, Lv) \leq \rho d(u, v) \quad (43)$$

with $d(\xi, \zeta)$ given by equation (41). The determination of the contraction of L at $u = u$ and $v = (u + \Delta u)$ is a representation that is thought of in operational calculus as the derivative of the operator L for vanishing Δu . Equation (43) is then written as:

$$d[Lu, L(u + \Delta u)] \leq \rho d[u, u + \Delta u] \quad (44)$$

If the vector u has m components and equation (44) is expanded using equation (41), the result is:

$$\frac{\left[|L(u_1+\Delta u)-Lu_1|^2 + |L(u_2+\Delta u)-Lu_2|^2 + \dots + |L(u_m+\Delta u)-Lu_m|^2 \right]^{\frac{1}{2}}}{\left[|u_1+\Delta u-u_1|^2 + |u_2+\Delta u-u_2|^2 + \dots + |u_m+\Delta u-u_m|^2 \right]^{\frac{1}{2}}} < \rho \quad (45)$$

Eliminating terms in the denominator of equation (45) yields:

$$\frac{\left[|L(u_1+\Delta u)-Lu_1|^2 + |L(u_2+\Delta u)-Lu_2|^2 + \dots + |L(u_m+\Delta u)-Lu_m|^2 \right]^{\frac{1}{2}}}{m|\Delta u|} < \rho \quad (46)$$

Now, since $m \geq 1$, a stronger condition is written

$$\frac{\left[|L(u_1+\Delta u)-Lu_1|^2 + |L(u_2+\Delta u)-Lu_2|^2 + \dots + |L(u_m+\Delta u)-Lu_m|^2 \right]^{\frac{1}{2}}}{|\Delta u|} < \rho \quad (47)$$

Consider the following: given

$$\left[|a_1|^2 + |a_2|^2 + \dots + |a_m|^2 \right]^{\frac{1}{2}} \leq |a_1| + |a_2| + \dots + |a_m| \quad (48)$$

Is the inequality true? Squaring both sides yields:

$$\begin{aligned} |a_1|^2 + |a_2|^2 + \dots + |a_m|^2 &\leq |a_1|^2 + |a_2|^2 + \dots + \\ &|a_m|^2 + |a_1||a_2| + |a_1||a_3| + \dots + |a_{m-1}||a_m| \end{aligned} \quad (49)$$

and the inequality is seen to be valid for non-zero a_i .

Equation (47) is then written as:

$$\frac{|L(u_1 + \Delta u) - Lu_1| + |L(u_2 + \Delta u) - Lu_2| + \dots + |L(u_m + \Delta u) - Lu_m|}{|\Delta u|} < \rho \quad (50)$$

and then may obviously be further reduced for each component

to:

$$\frac{|L(u_i + \Delta u) - Lu_i|}{|\Delta u|} \leq \rho_i \quad (51)$$

noting that $\sum_{i=0}^m \rho_i < \rho$.

From equation (51) it is seen that a complex-valued ρ_{c_i} may be defined and the final form of equation (51) becomes:

$$\frac{L(u_i + \Delta u) - Lu_i}{\Delta u} = \rho_{c_i} \quad (52)$$

This form is the measure of the derivative of the operator L at each component and may be used to solve for the contraction corrector R_i at each component $u_i \in u$.

Even though a powerful tool has been developed to allow the computation of a convergent one-dimensional solution to electromagnetic scattering, the background problems surrounding the contraction corrector scheme should be examined. This background material is of interest since the breakdown of prior methods and the reasons for non-convergent solutions gives insight into what particulars of the scattering problem cause the difficulties. In particular, known geometrical problem areas are: conductor width, cell size, aperture size, and the angle of incidence and polarization of the impinging plane wave. The understanding of the difficulties arising for certain values of those parameters can provide vital insight when attempting to extend the solution to two-dimensional configurations, especially when mesh structures are involved. The reference point for this background investigation is the work of Tsao and Mittra [9]. A complete iterative flow is detailed in Appendix B.

Consider the case of the free-standing strips shown in Figure 3. This planar configuration of thin, perfect conductors was the prime example used in the work of Tsao and Mittra [9]. The case of a cell width of 1.4λ , aperture width of 0.6λ , and incidence angle $\theta=0^\circ$ was of particular interest. Although the iteration equation (40), would perform adequately, Tsao and Mittra decided to apply a correction step to the iterative process. The idea of being "near" the solution in numerical methods (i.e., Newton's

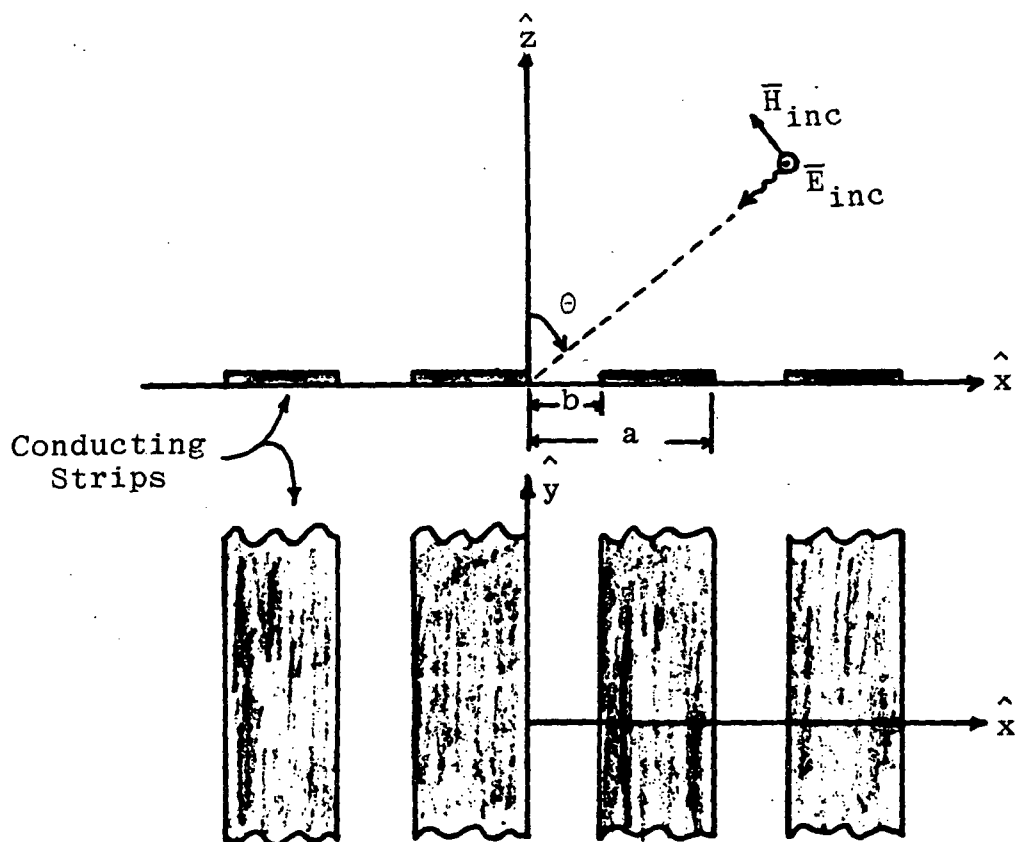


Figure 3. Free-standing conducting strips with Floquet cell width a , aperture size b and conductivity σ .

Method) to either insure or speed convergence is common place. The correction step was chosen to be a form of the Method of Moments [28] .

The amount of amplitude error of $\bar{E}^{(n+1)}$ may be calculated from processing $\bar{E}^{(n)}$ with equation (40) and using an amplitude correction C determined via a variational formula calculated with Galerkin's method. This correction is given by [9] :

$$C = \left| \frac{\langle \bar{E}_{\text{tan}}^{(n)}, -\bar{H}_{\text{tan}}^i \rangle}{\langle \bar{E}_{\text{tan}}^{(n)}, F^{-1} G \cdot \bar{E}_{\text{tan}}^{(n)} \rangle} \right| \quad (53)$$

where:

$$\langle \bar{x}_1, \bar{x}_2 \rangle = \int_{\text{aperture}} \bar{x}_1 \times \bar{x}_2^* \cdot d\bar{s} \quad (54)$$

with "*" denoting conjugation and $d\bar{s}$ the outward surface normal. The value of C yields a weighted average error based on the first moment's variation of the operator using $\bar{E}^{(n)}$ as the test function. C will be equal to one when $\bar{E}^{(n)}$ represents the averaged approximate solution to the problem. This statement implies that oscillations of the solution could average out and yield a solution that is incorrect.

Numerical difficulties could then arise if a problem generated such a solution from the iterative process. Great care is then warranted with this type of numerical method as is true with any numerical scheme. Additionally, as previously noted for iterative processes, just being near the correct solution in amplitude does not guarantee a convergent process.

The geometry given in Figure 3 for $a=1.4\lambda$, $b=0.6\lambda$, $\theta=0^\circ$ and \bar{H} -wave (\bar{E}_{tinc} parallel to strip edges) incidence is a problem that converges by equation (40) without the aid of the variational correction of equation (53). What then is the useful purpose of the correction C? The most useful purpose of C is to speed convergence since an iterative equation which is a contraction will converge from any initial estimate and will diverge if not a contraction. Another useful (but applied with caution) purpose is the indication of accuracy of the iterated solution. The problem above is taken from Tsao and Mittra [9]. The convergence of the problem is shown in Figure 4. Figure 5 illustrates the convergence of $\bar{E}^{(n)}$ of the problem using equation (40) corrected by C of equation (53). The iterations of both Figure 4 and Figure 5 are quite similar; however, the $\bar{E}^{(n)}$ shown in Figure 5 are converging more rapidly than the $\bar{E}^{(n)}$ in Figure 4 by one iteration. This is a very small difference in convergence rates and indicates that the methods behave similarly.

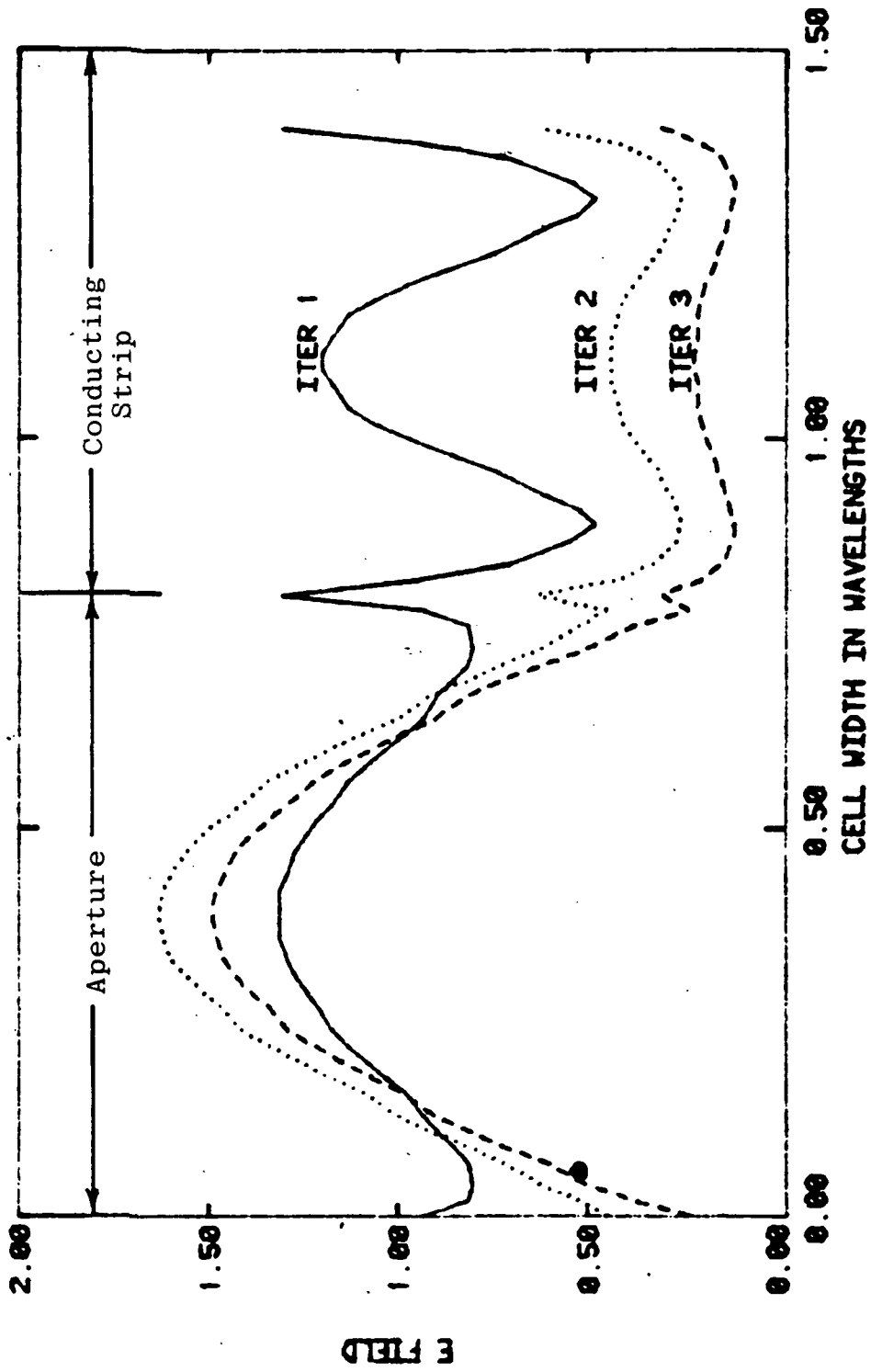


Figure 4. Convergence of the aperture \bar{E} field for $a=1.4\lambda$, $b=0.6\lambda$, $\theta=0^\circ$ case using equation (40).

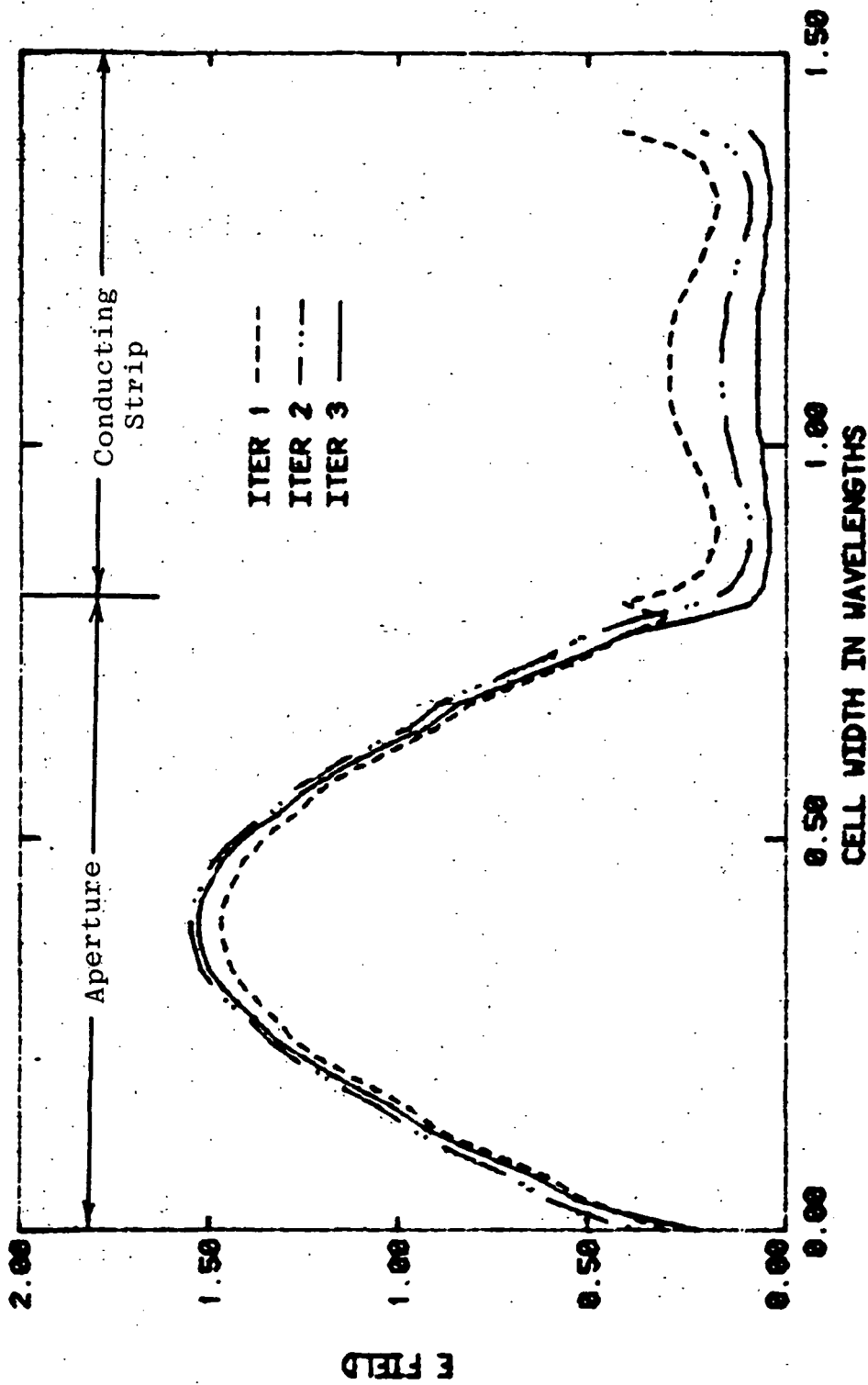


Figure 5: Convergence of the aperture \bar{E} field for $a=1.4\lambda$, $b=0.6\lambda$, $\theta=0^\circ$ case using equation (40) with the correction of equation (53) applied, from Tsao and Mittra [9].

Equation (42) is also used to solve the problem above. The contraction corrector \bar{R} is obtained using equation (52) along with equation (34). The application of this contraction corrector yields results for $\bar{E}^{(n)}$ shown in Figure 6. Note that the first iteration is the same as the first iteration in Figure 4. However, the second and third iterations shown in Figure 6 are improved over those in Figure 5. Even though this convergence improvement is by one iteration, it is pointed out that the contraction corrector guarantees convergence (except for possible numerical computational problems). The case for using the contraction corrector over the other methods is not well presented in the preceding example. The basic iterative equation and the variational corrected iterative equation break down and diverge for various cases. The following material is presented to establish bounds for the regions of solvability for the preceding problem and to demonstrate the usefulness of contraction theory in this matter.

The basic iterative formulation is found lacking for various cases. Conductor size, aperture size, cell size and incidence angle are the parameters that are varied and may cause convergence difficulties. The first case to be examined is that of constant Floquet cell width and varying aperture size. In particular, let $a = 1.4\lambda$ and $0.005\lambda \leq b \leq 1.395\lambda$ for perfectly conducting strips, incident angle $\theta=0^\circ$ and H-wave polarization. The contraction factor for this

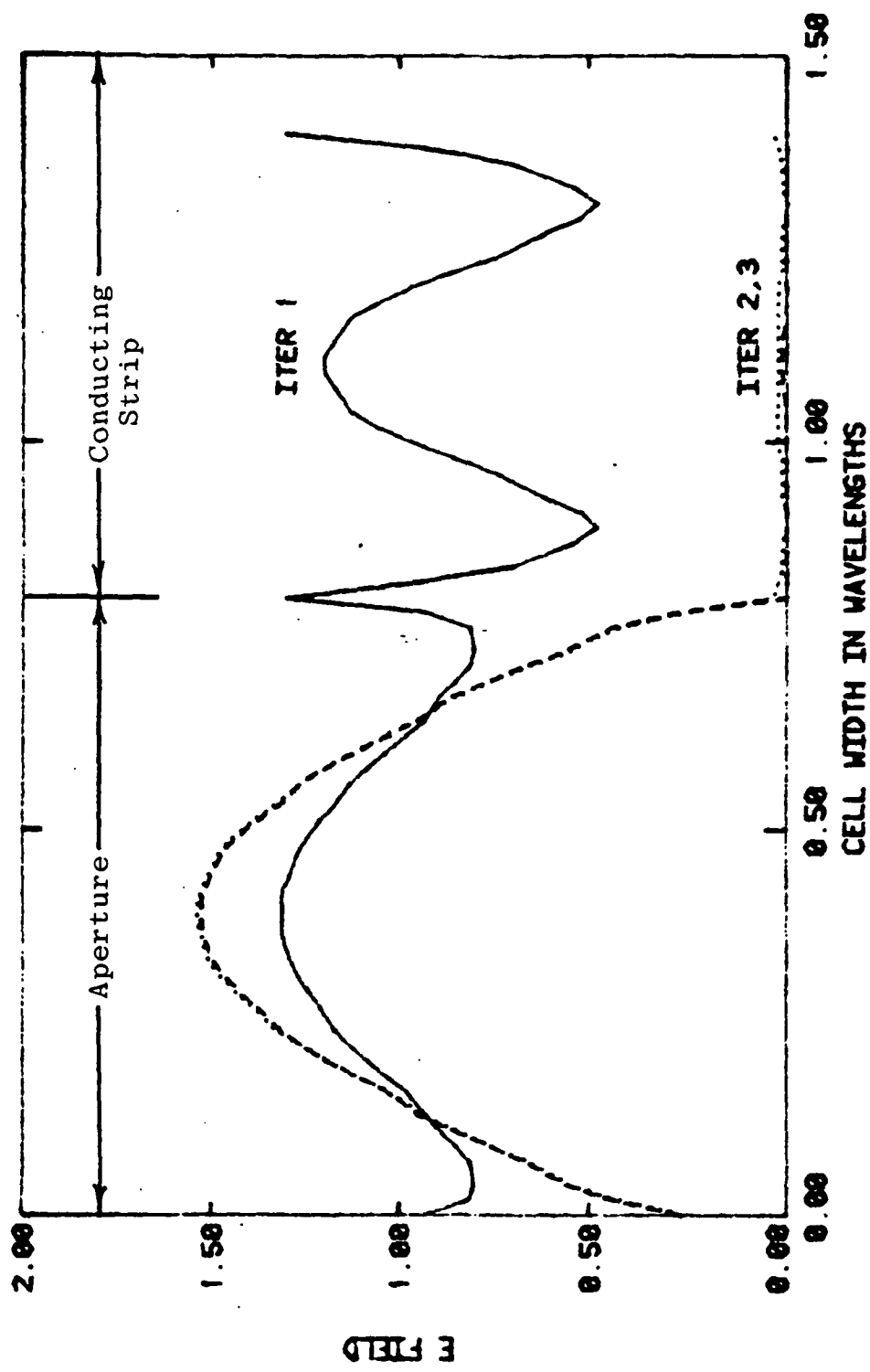


Figure 6. Convergence of the aperture \bar{E} field for $a=1.4\lambda$, $b=0.6\lambda$, $\theta=0^\circ$ case using equation (42). This is the contraction corrector method.

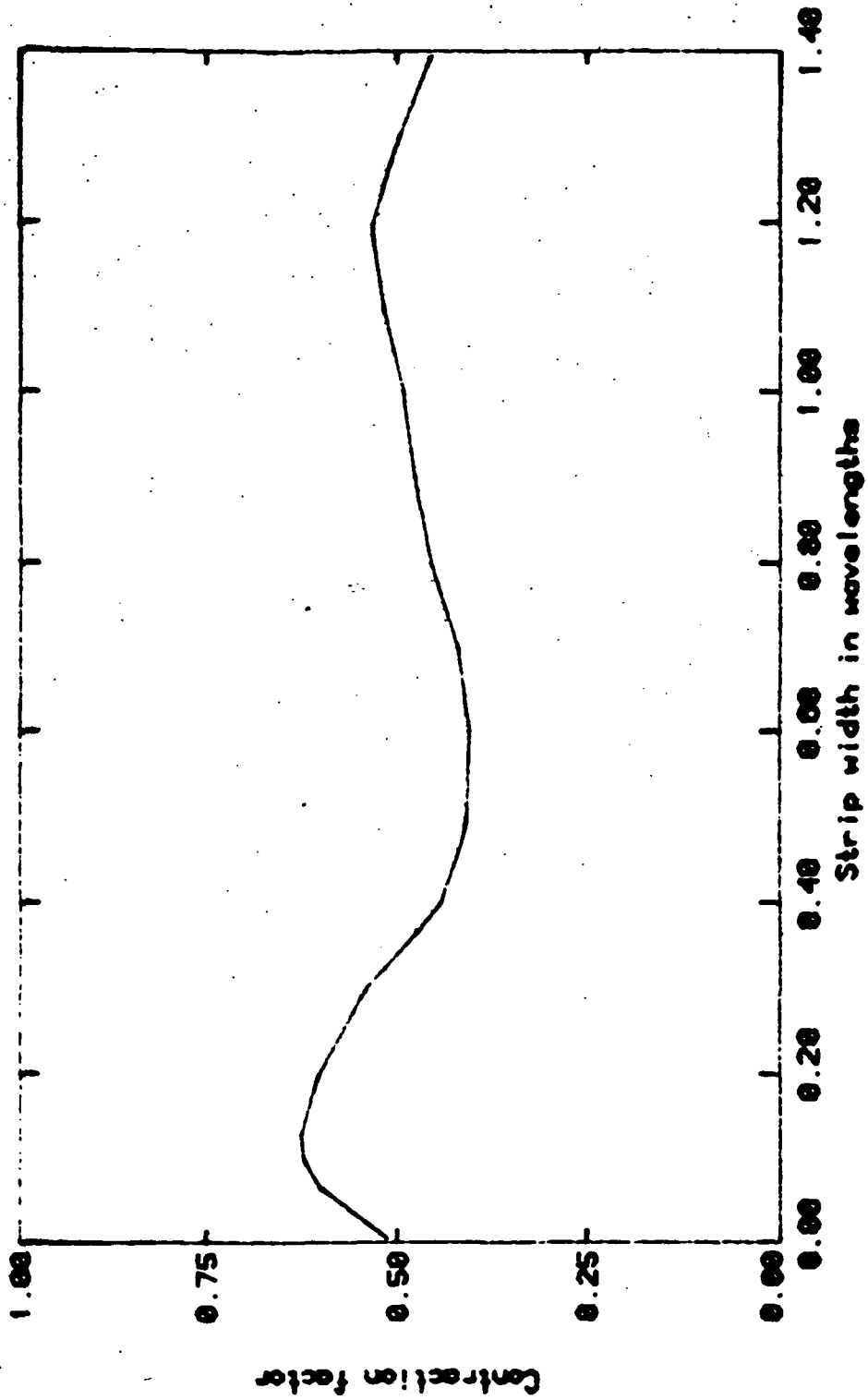


Figure 7. Contraction factor for a cell width of 1.4λ , incidence

angle $\theta=0^\circ$ with H-wave polarization and $\phi=0^\circ$.

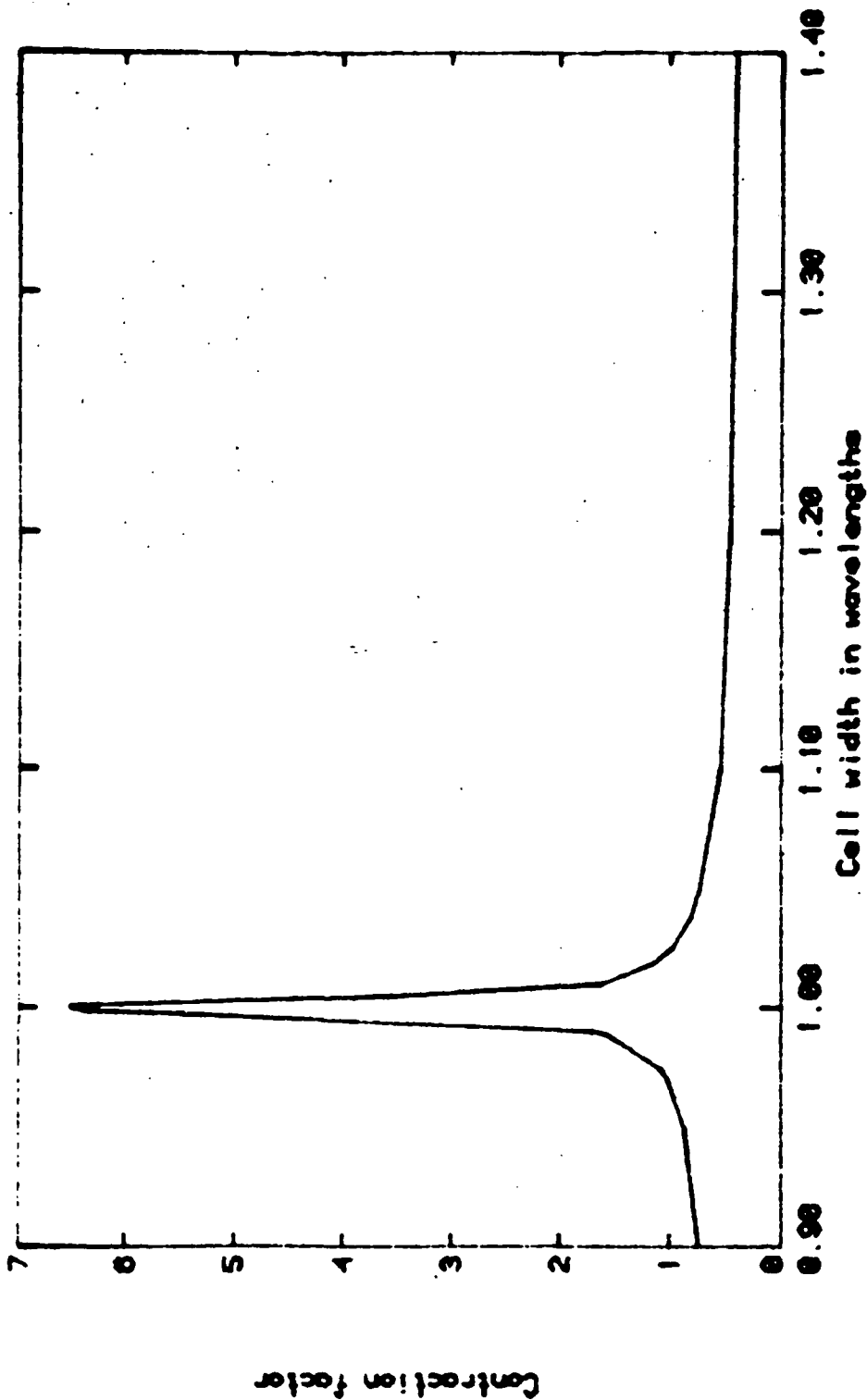


Figure 8. Contraction factor for a strip width of 0.6λ , incidence angle $\theta=0^\circ$ with H-wave polarization and $\phi=0^\circ$.

case is graphed in Figure 7. Recall that the solution will diverge for a contraction factor greater than one. These non-convergent regions are where the contraction corrector must be applied to insure convergence. Next, the cell size is varied as $0.9\lambda \leq a \leq 1.4\lambda$ for constant conductor size, i.e., $(a-b) = \text{constant}$, and $\theta = 0^\circ$ with H-wave polarization. Figure 8 shows the contraction factor for a conductor size 0.8λ . This last example contained a conducting strip that was a large portion of a wavelength. The case of a conductor size 0.1λ and cell width $0.2\lambda \leq a \leq 0.9\lambda$ for H-wave polarization and $\theta = 0^\circ$ is presented in Figure 9. This example represents a small strip and the contraction factor associated with its geometry. The last case to be examined is concerned with the angle of incidence of the impinging plane wave. A cell width $a = 0.9\lambda$, conductor width $b = 0.4\lambda$ and aperture width 0.5λ is chosen for the convergence survey illustrated in Figure 10. Note that the contraction factor bumps above 1.0 around $\theta = 8^\circ$ and diverges from 1.0 for $\theta > 60^\circ$. This indicates that the basic iterative scheme will have problems with convergence around $\theta = 8^\circ$ and will not converge for $\theta > 60^\circ$. The above examples offer several cases that point out problem areas in constructing a convergent iterative solution.

The contraction corrector may be applied to construct a convergent solution when the basic iterative scheme

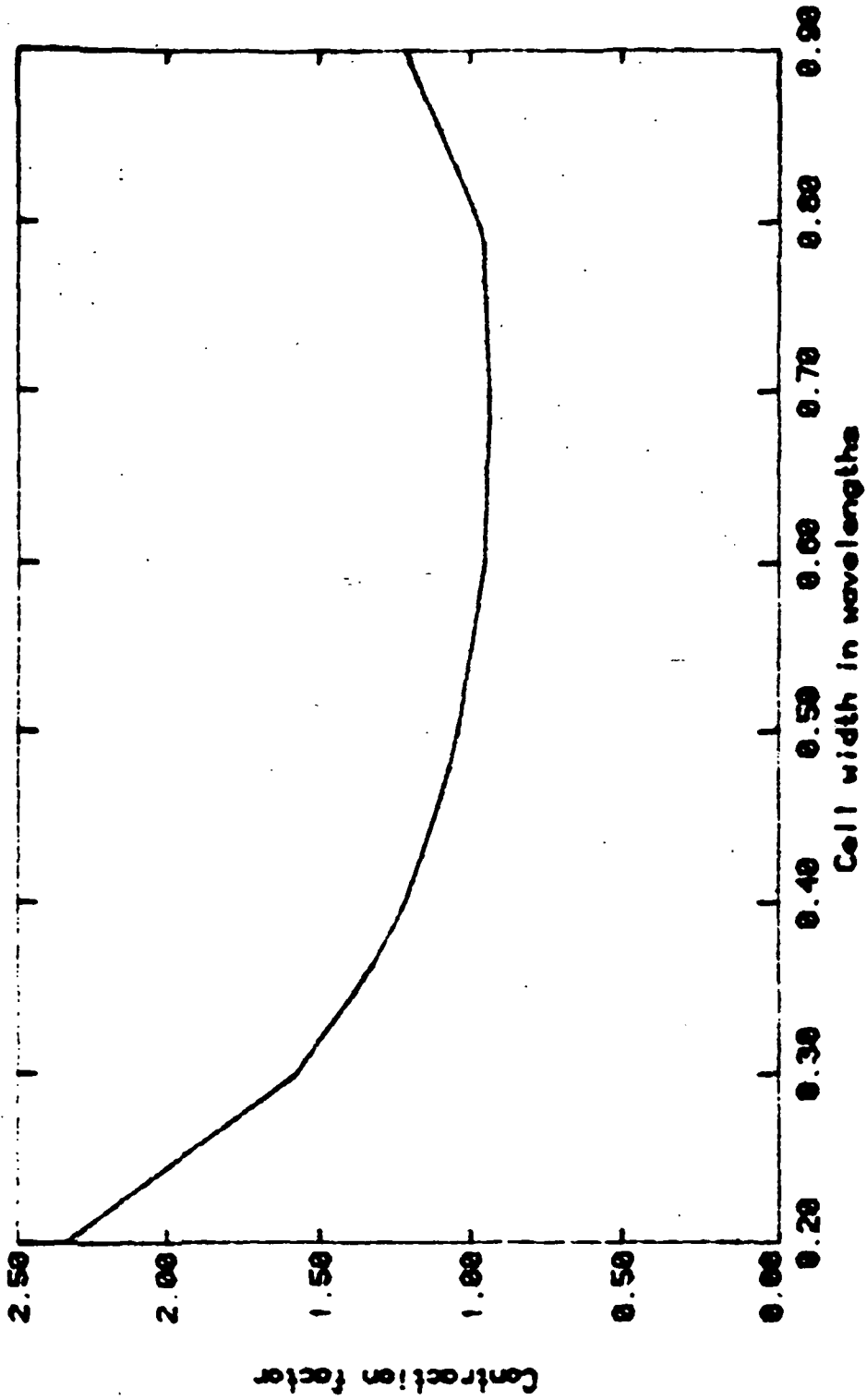


Figure 9. Contraction factor for a strip width of 0.1λ , incidence angle of $\theta=0^\circ$ with H-wave polarization and $\phi=0^\circ$.

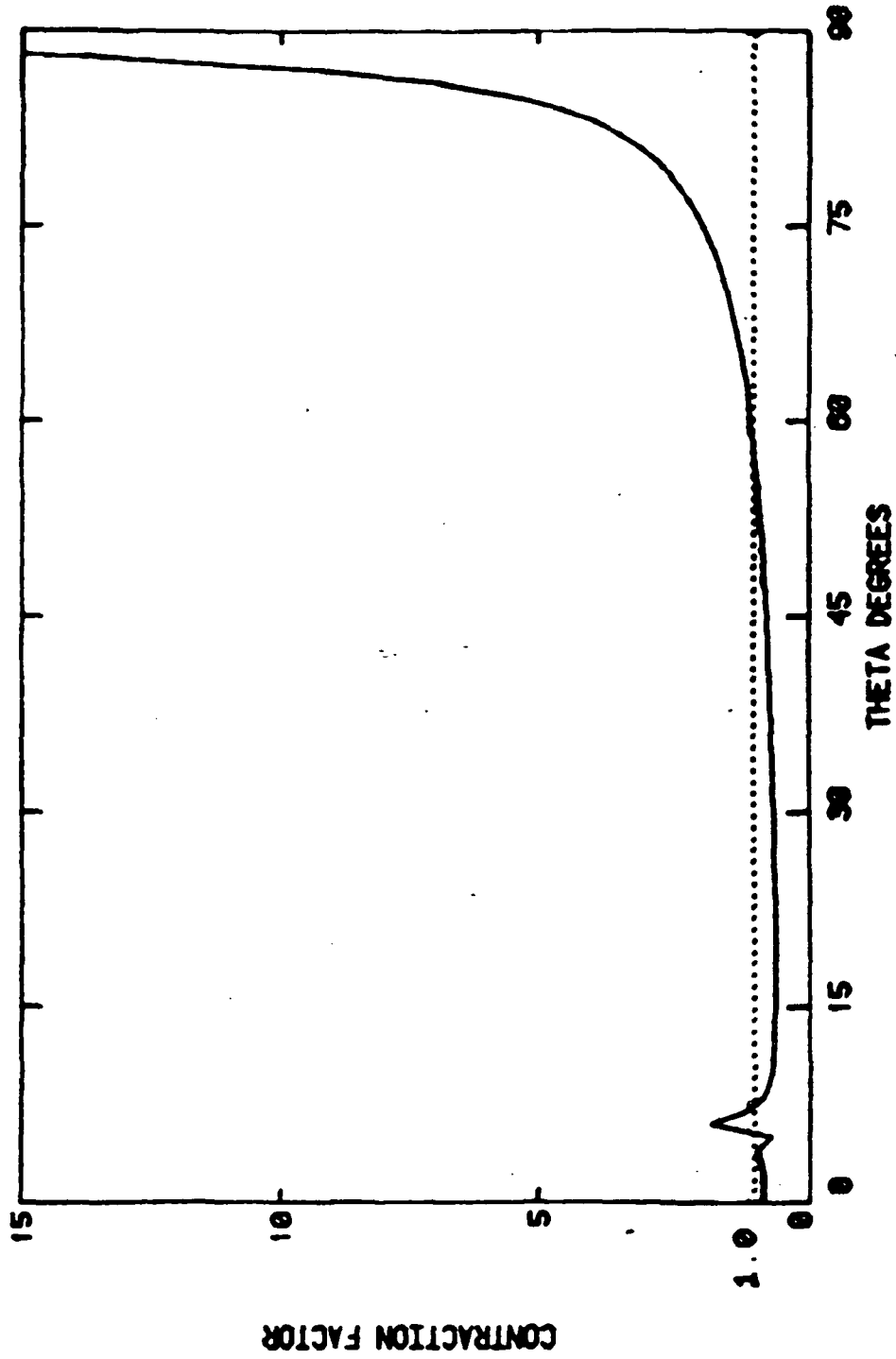


Figure 10. Convergence survey using contraction criteria for $0^\circ < \theta < 90^\circ$, $\phi = 0^\circ$, $a = 0.9\lambda$, and $b = 0.4\lambda$.

breaks down. Consider the case of Figure 3 with $a = 1.4\lambda$, $b = 0.6\lambda$ and $\theta = 70^\circ$. At this incidence angle, the iteration equation (40) and variational correction of Tsao and Mittra [9] break down and do not converge. Figure 11 illustrates that after six and seven iterations respectively, neither method converges. However, Figure 12 reveals that the contraction corrector method converges after six iterations and has a small error over the conductor. Herein lies the reason the contraction corrector method is preferred. Even when the basic method and variational correction schemes fail to converge, the contraction corrector method assures that solution can be reached and does so with reasonable ease.

The foregoing examples have demonstrated the ability of the contraction criteria to be applied to one-dimensional scattering problems to determine the regions of solvability. Additionally, the contraction corrector scheme has been utilized to achieve convergence when the basic iterative schemes failed. The examples presented give indications that the contraction corrector can be successfully applied to planar wire surfaces.

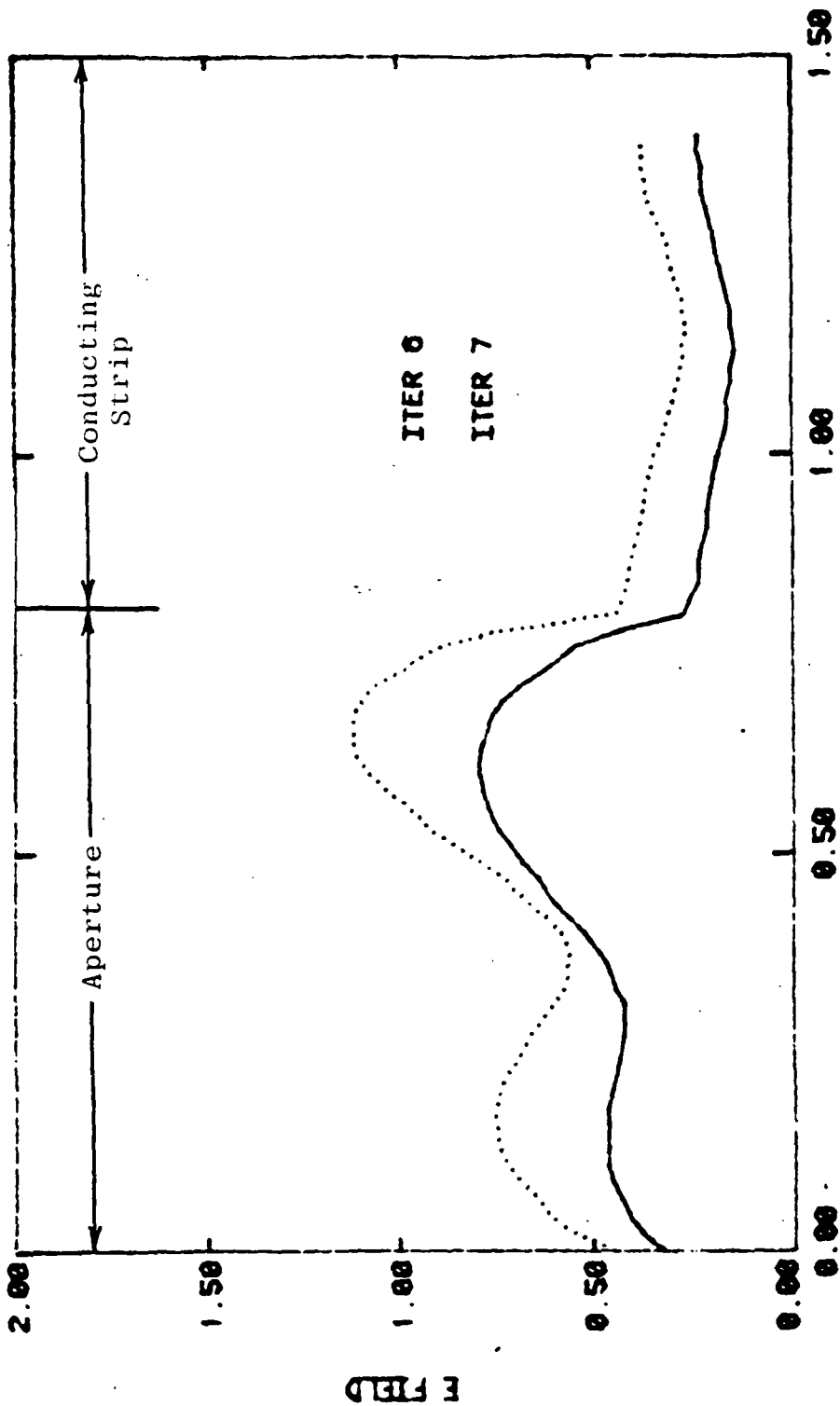


Figure 11a. Non-convergent results of the variational corrected iterative equation for $\theta=70^\circ$.

ORIGINAL PAGE IS
OF POOR QUALITY

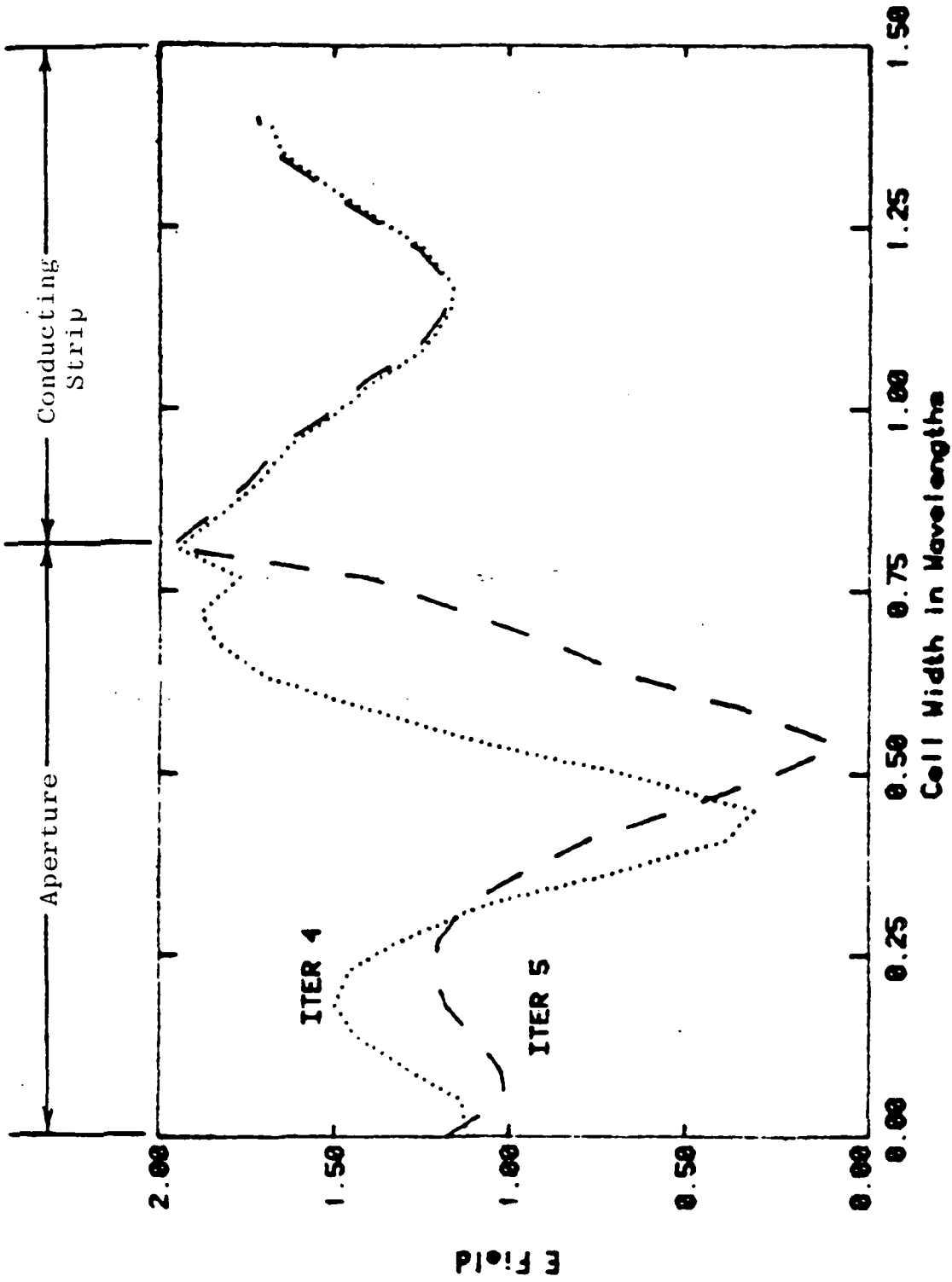


Figure 11b. Non-convergent results for the basic iterative equation with $\theta=70^\circ$.

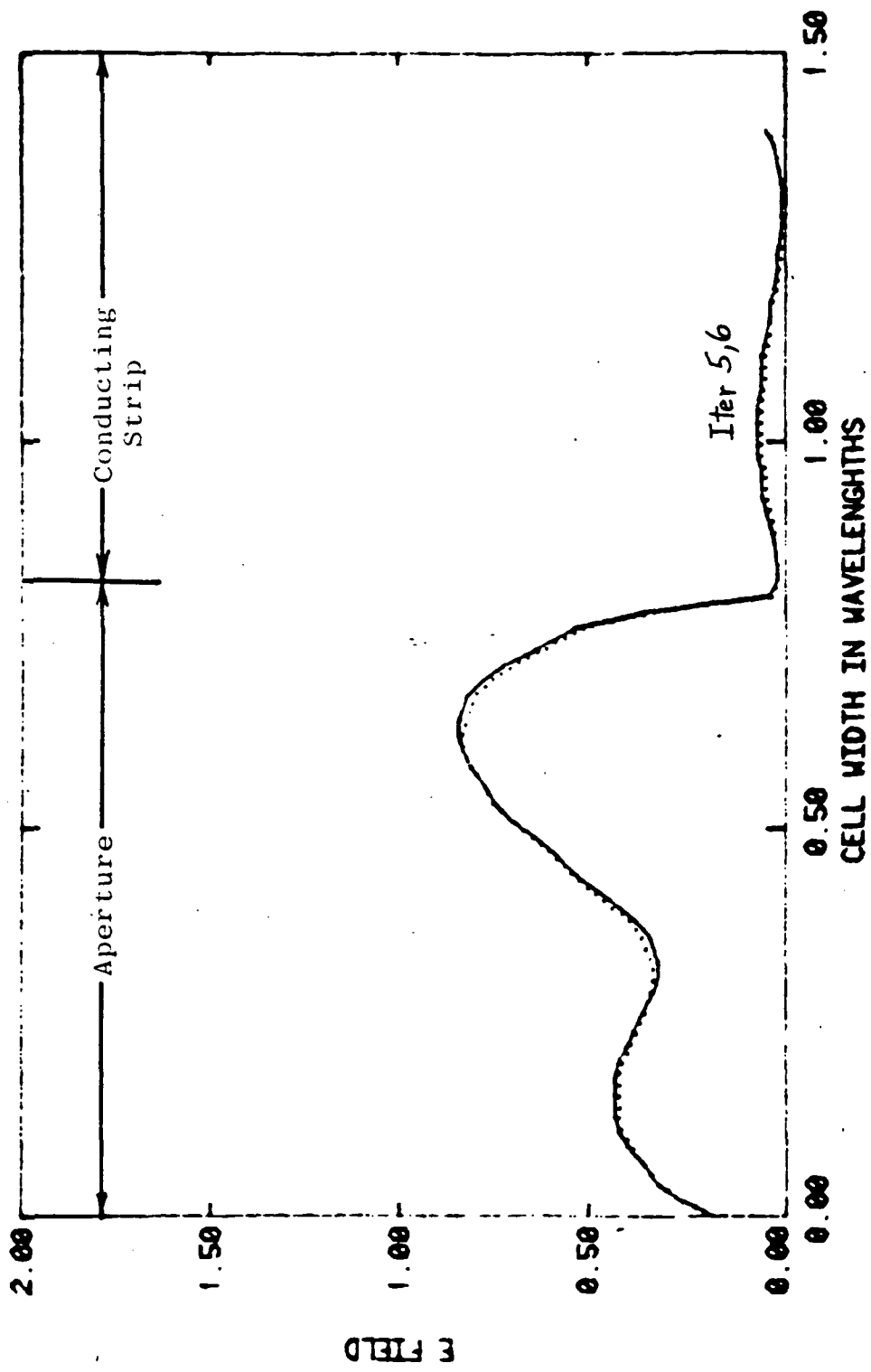


Figure 12. Convergent results obtained from the contraction corrector method of equation (30) with $\phi=0^\circ$, $\theta=70^\circ$, $a=1.4\lambda$ and $b=0.6\lambda$.

V. THE PROBLEM OF AN INFINITE GRATING
OF THIN WIRES

The structure shown in Figure 13 has been studied over the years by various techniques to determine the reflection coefficient from the grid [1, 2, 20]. The reflection coefficient may be obtained from the transform of the aperture \bar{E} field in the form of the Floquet modes. For the case of cell widths less than $\lambda/2$, this coefficient is obtained from the $n = m = 0$ element of the $E_{y\ mn}^-$ variable for the case of plane wave incidence as [9]

$$\Gamma = \frac{\tilde{E}_{y00}^-}{\tilde{E}_{y00}^+} = \frac{\tilde{E}_{y00}^-}{\tilde{E}_{y00}^+} - E_{yinc} \quad (55)$$

The first attempt to solve the problem with a $\lambda/4$ cell and $\lambda/600$ radius wire was performed with the variational correction iterative process using $\bar{E}^{(n)}$ as a test function in the variational scheme. This method fails to converge for various sampling rates and various numbers of Floquet modes, and a more suitable test function is sought [21]. The Dirac delta function is chosen as the test function and gives acceptable results for small angles of incidence. The delta function samples the response and allows point matching to be utilized to improve the variational correction factor. The convergence properties achieved with these two test functions are shown in Figure 14. Since the iteration method should be convergent for all incidence angles,

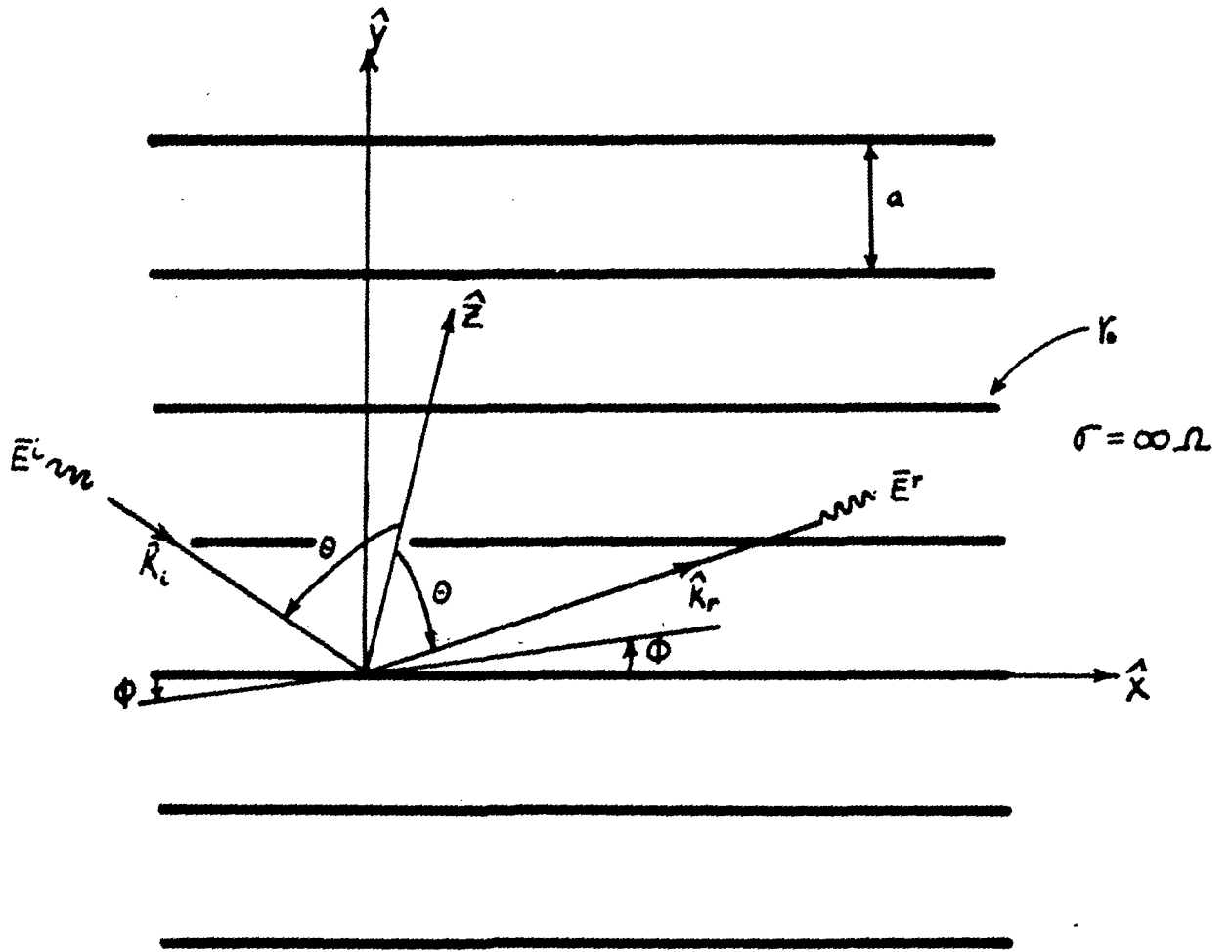


Figure 13. Planar grid of thin conducting wires.

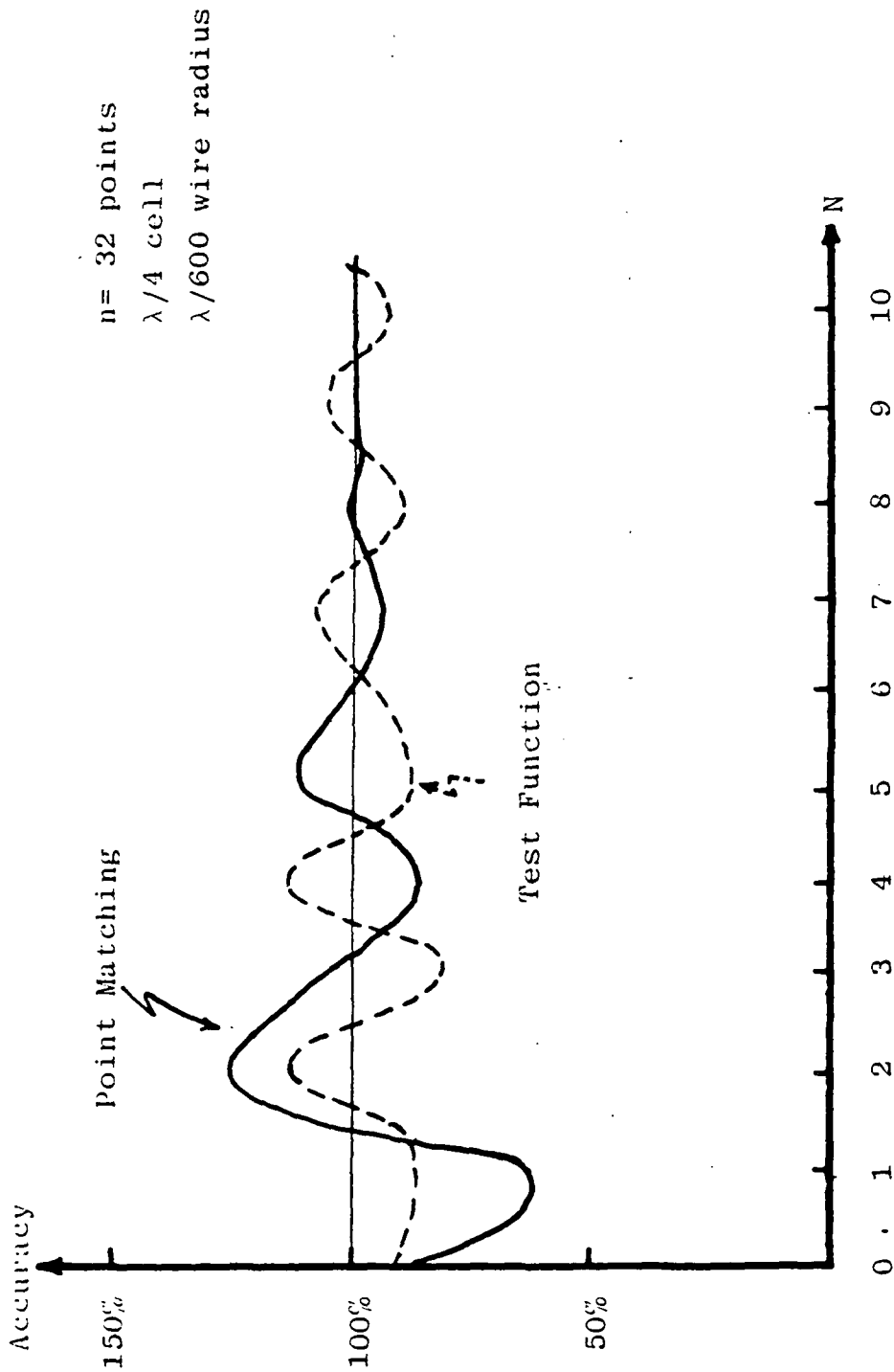


Figure 14. Convergence properties of the variational correction scheme using both $\bar{E}(n)$ and the Dirac delta function as the test function with $\phi = \theta = 0^\circ$, $a = 0.25\lambda$ and $b = 0.247\lambda$.

the development of a different form of correction is a logical path to follow.

The iterative process of equation (40) is one derived for \bar{E} from itself. That is, the $\bar{E}^{(n+1)}$ was determined from $\bar{E}^{(n)}$ with an intermediate step in the iterative process used to determine the surface current density $\bar{J}^{(n)}$. The iterative process then has two distinct parts and it is reasoned that two distinct correction factors are required. By weighting previous iterations of both $\bar{E}^{(n)}$ and $\bar{J}^{(n)}$, it is found that convergence can be obtained for small cell size and near normal angles of incidence. However, it is also determined that the stability and speed of convergence is critically dependent on the weights chosen. It is then realized that a solution may only be obtained by an "accident" as mentioned before. The hit-and-miss approach required by the weighted iterations may allow the determination of a proper solution but the recursive time required could be excessive. These facts then drive the iteration equation toward a solution obtained by the contraction corrector method.

The cases chosen for examination are $\lambda/8$, $\lambda/4$, and $\lambda/2$ cell widths with both TE and TM incidence. The TE case corresponds to incidence angles $\phi = 0^\circ$ and $0^\circ \leq \theta \leq 90^\circ$ while the TM case corresponds to incidence angles $\phi = 90^\circ$ and $0^\circ \leq \theta \leq 90^\circ$, with either \bar{E}_{inc} or \bar{H}_{inc} respectively co-

polarized to the wires. Since the determination of reflection from two-dimensional mesh reflector antenna surfaces is the application toward which this work is directed, the reflection coefficients must be carefully scrutinized to ascertain the best definition of reflection. Wait [2] defines a suitable normal reflection coefficient and a comparison to his results will be made. The specular reflection is of interest in antenna work and the construction of the geometry required is given in Figure 15 [22]. When \bar{E}_{inc} is entirely co-polarized with the grid wires, the two reflection coefficients agree in definition. With TM polarization (vertical) incident, a pseudo-Brewster angle is expected at certain incidence angles. Variations of magnitude are also expected to occur with changing wire conductance. Before examining various cases and comparing the results to those of previous authors, the wires must be converted into equivalent strips to yield a structure equivalent to that used by the previous authors [1, 2, 20, 27].

Harrington [29] relates that equivalence between thin metallic rectangular strips and small radius wires is obtained if

$$b = 4w \quad (56)$$

where b = radius of the wires and w = width of the strips. Thus, using equation (56), we are able to use the strip ana-

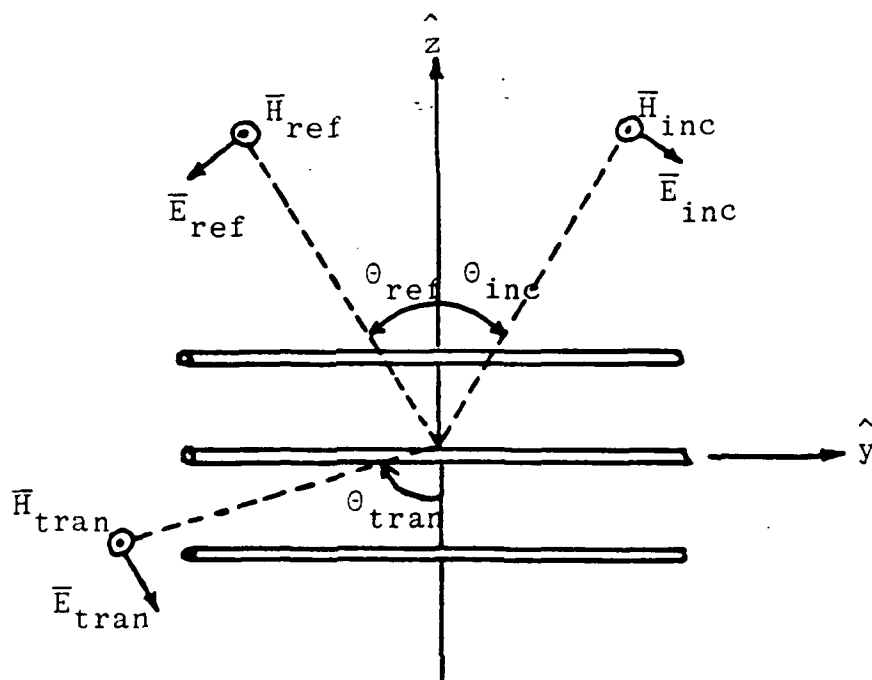
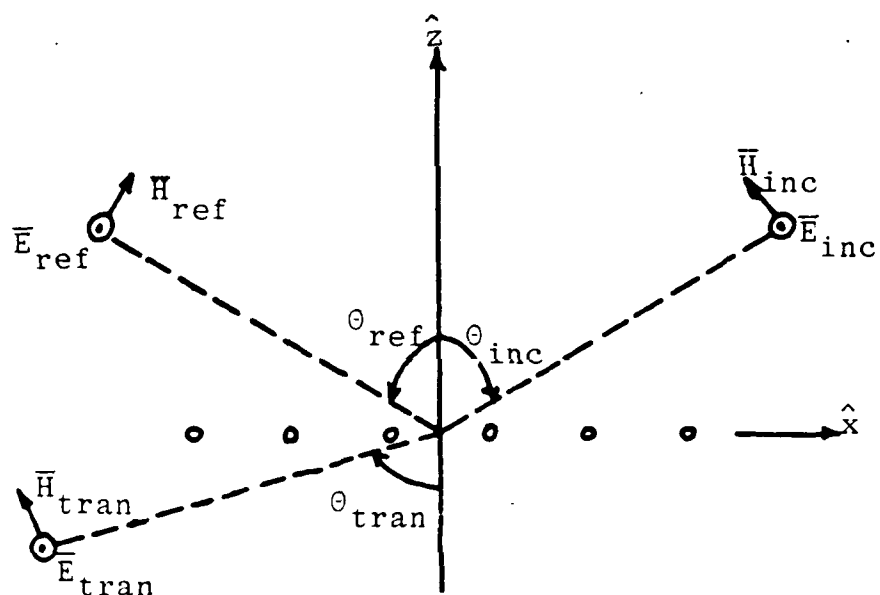


Figure 15. Definition of reflection coefficients as described in [22].

lysis to determine the reflection from a grid of cylindrical wires. A further characterization of the wires is required when the wires are of finite conductivity. Schelkunoff [23] gives the internal impedance of a thin cylindrical wire as

$$Z_{\text{int}} = \frac{\eta_m K_0(\gamma b)}{2\pi b K_1(\gamma b)} \quad (57)$$

where $\eta_m = j\mu_m\omega / (\sigma_m + j\omega\epsilon_m)^{1/2}$ and $\gamma = j\mu_m\omega(\sigma_m + j\omega\epsilon_m)^{1/2}$ with μ_m, ϵ_m , and σ_m being the electrical properties of the wire and K_0, K_1 being modified Bessel functions. These principles may now be applied to the cases detailed above.

The cases of cell widths of $\lambda/8$, $\lambda/4$, and $\lambda/2$ are now presented with a wire radius of $\lambda/600$. Good agreement is obtained between the results of the contraction correction method and the results of Wait [2] for incidence angles of both $\phi = 0^\circ$ and $\phi = 90^\circ$. The case of $\phi = 0^\circ$ is illustrated in Figure 16. Recalling the other definition of reflection coefficient given in Figure 15, the reflection coefficients for the case of $\phi = 90^\circ$ are shown in Figure 17. The expected pseudo-Brewster angle is observed as a reflection minimum near the angle of 67° . The internal impedance of the wire becomes important in the problem when the conductivity of the wires becomes finite. Instead of the tangential electric fields cancelling over the conducting portion of the cell, they must combine to support the current at the

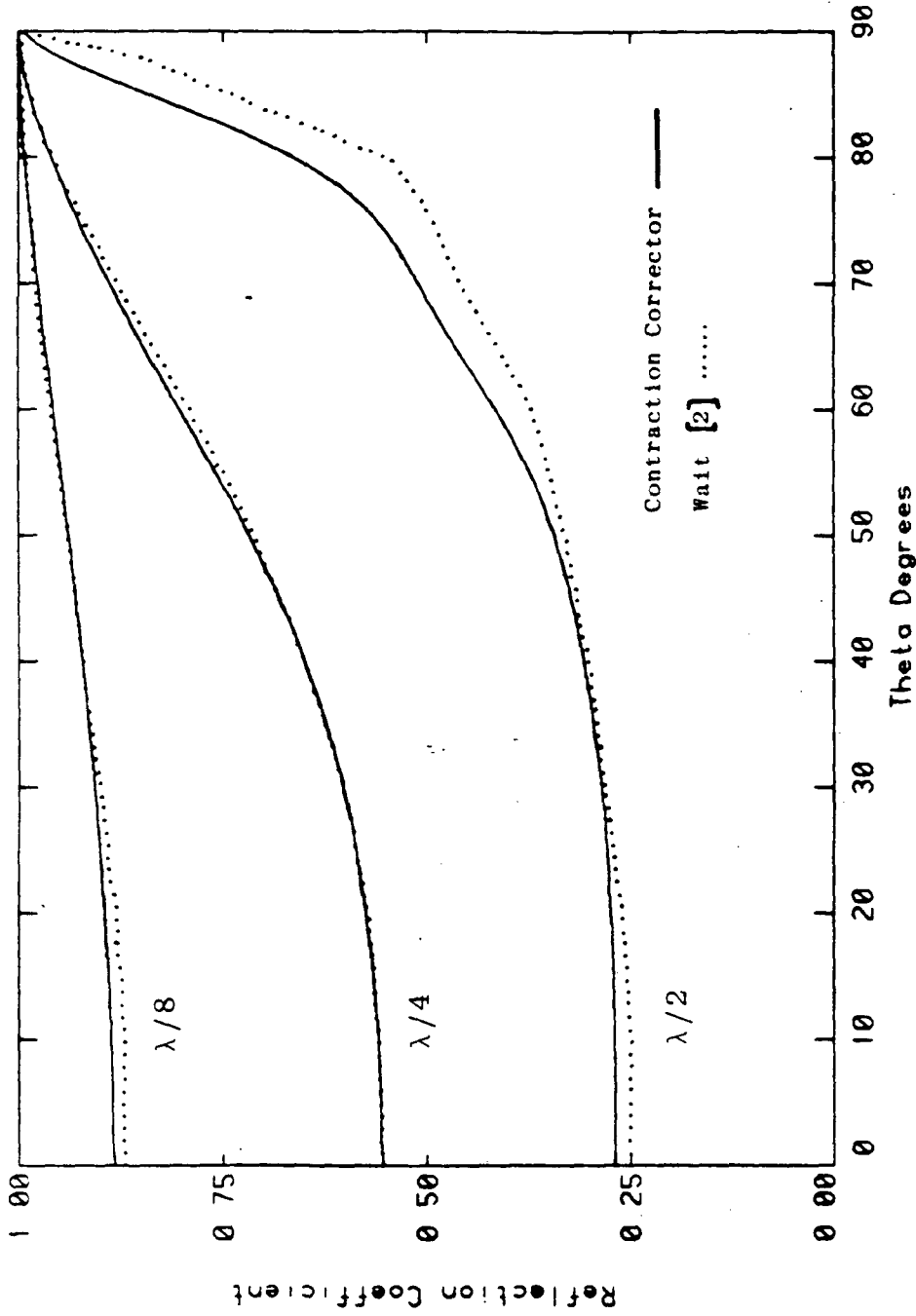


Figure 16. Comparison of results obtained from Wait [2] and equation (30) for various cell widths with $\phi=0^\circ$, $0^\circ \leq \theta \leq 90^\circ$, and $\sigma = \infty$ S.

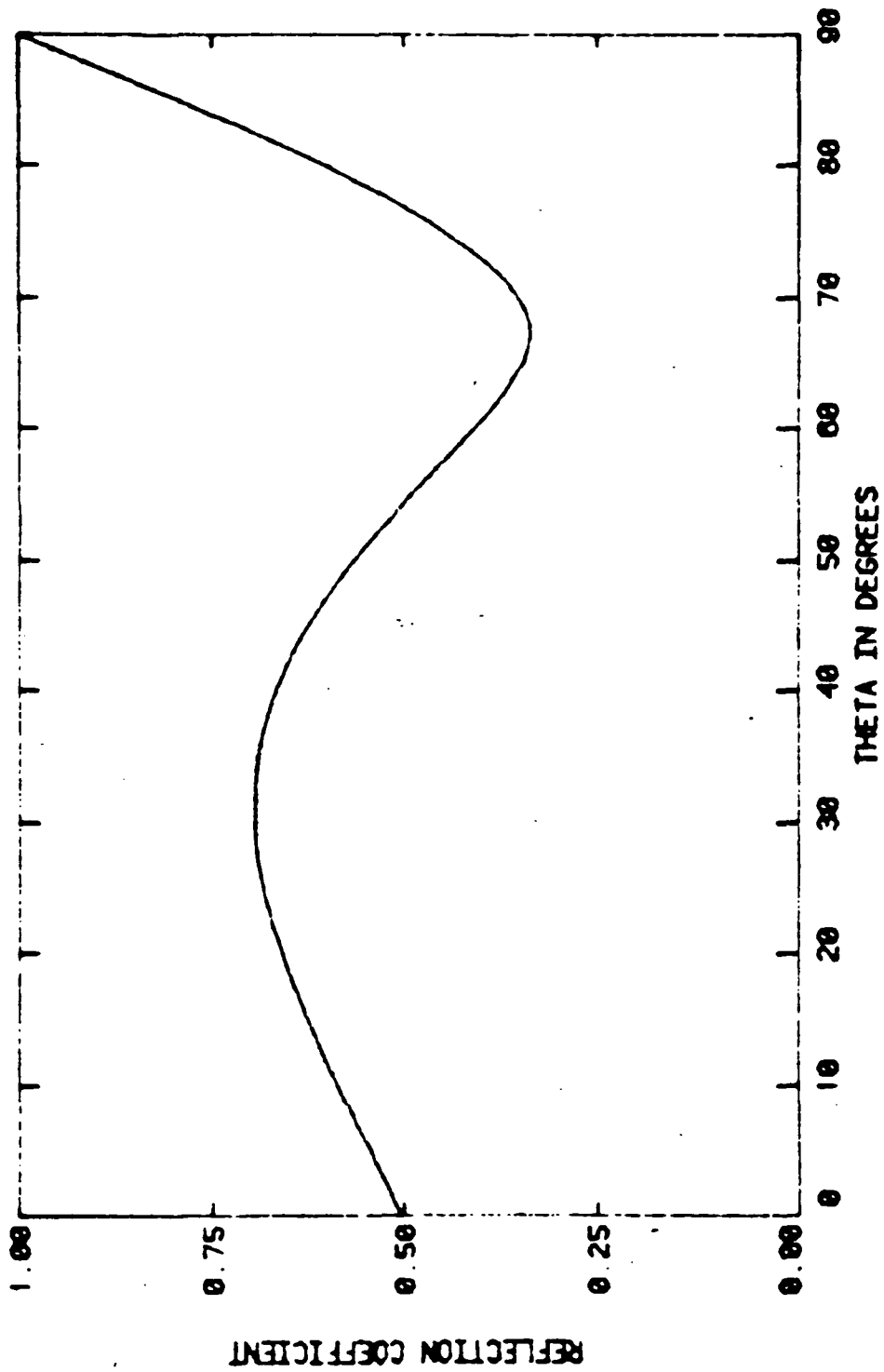


Figure 17. Reflection coefficient as defined in Figure 15 for $\phi=90^\circ$, $0^\circ < \theta < 90^\circ$, $a=0.25\lambda$, $b=0.247\lambda$ and $\sigma = \infty$ S.

surface as

$$\bar{E}_{\text{tinc}} + \bar{E}_{\text{tscat}} = \bar{I}_0 Z_{\text{int}} \quad (58)$$

where \bar{E}_{tscat} = scattered electric field and \bar{I}_0 = current along the conductor. The results of a finite conductivity are shown in Figure 18 where equation (58) has been included in the iteration equation. The results resemble that given by Jordan and Balmain [30] for a lossy ground and follow the idea that the grid represents a shunt impedance. Overall, good agreement is obtained with previously computed and measured results.

As a final note, some concern has been expressed over the non-convergence of the iterative technique and over the fact that increasing the number of Floquet modes not increase the accuracy of the solution [24]. The first concern has been addressed in the preceding sections while the second will be addressed now. When an iterative equation is in a non-convergent region, the solution may only be arrived upon by an accident of computation unless special methods of computation have been included.

The consequence of adding additional Floquet modes is adding additional points that are in the non-convergent region. The result of this consequence can range from producing a large variation in the iterated solution to helping

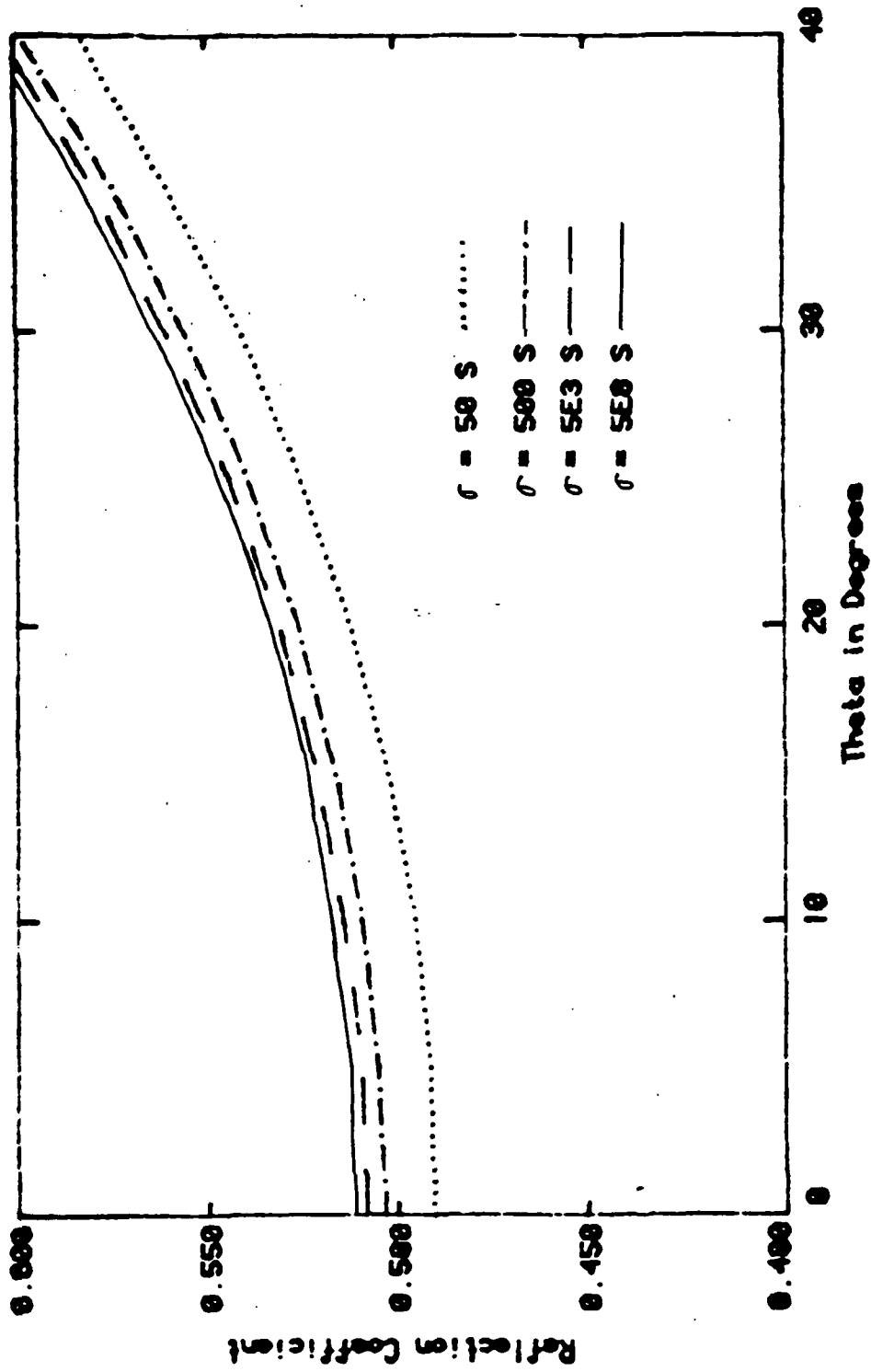


Figure 18. Several cases of finite conductivity with $\phi=0^\circ$, $0^\circ \leq \theta < 90^\circ$, $a=0.25\lambda$ and $b=0.247\lambda$.

the iterated solution. The control over the results is nil with a non-convergent iterative scheme. However, when the contraction corrector method is applied, the expected increase in accuracy with increasing Floquet modes is obtained. Of course, a limit on accuracy still exists due to the finite register length of the computing machine used. The case of a $\lambda/4$ cell width, $\lambda/600$ radius wire with infinite conductivity and $\phi = \theta = 0^\circ$ is chosen to illustrate the above comments. A plot of converged accuracy is shown in Figure 19. The usual leveling off accuracy is noted. This is due to the higher order Floquet modes having less and less effect on the solution, i.e., the farther away wires contribute less and less to the fundamental cell when a convergent process is used.

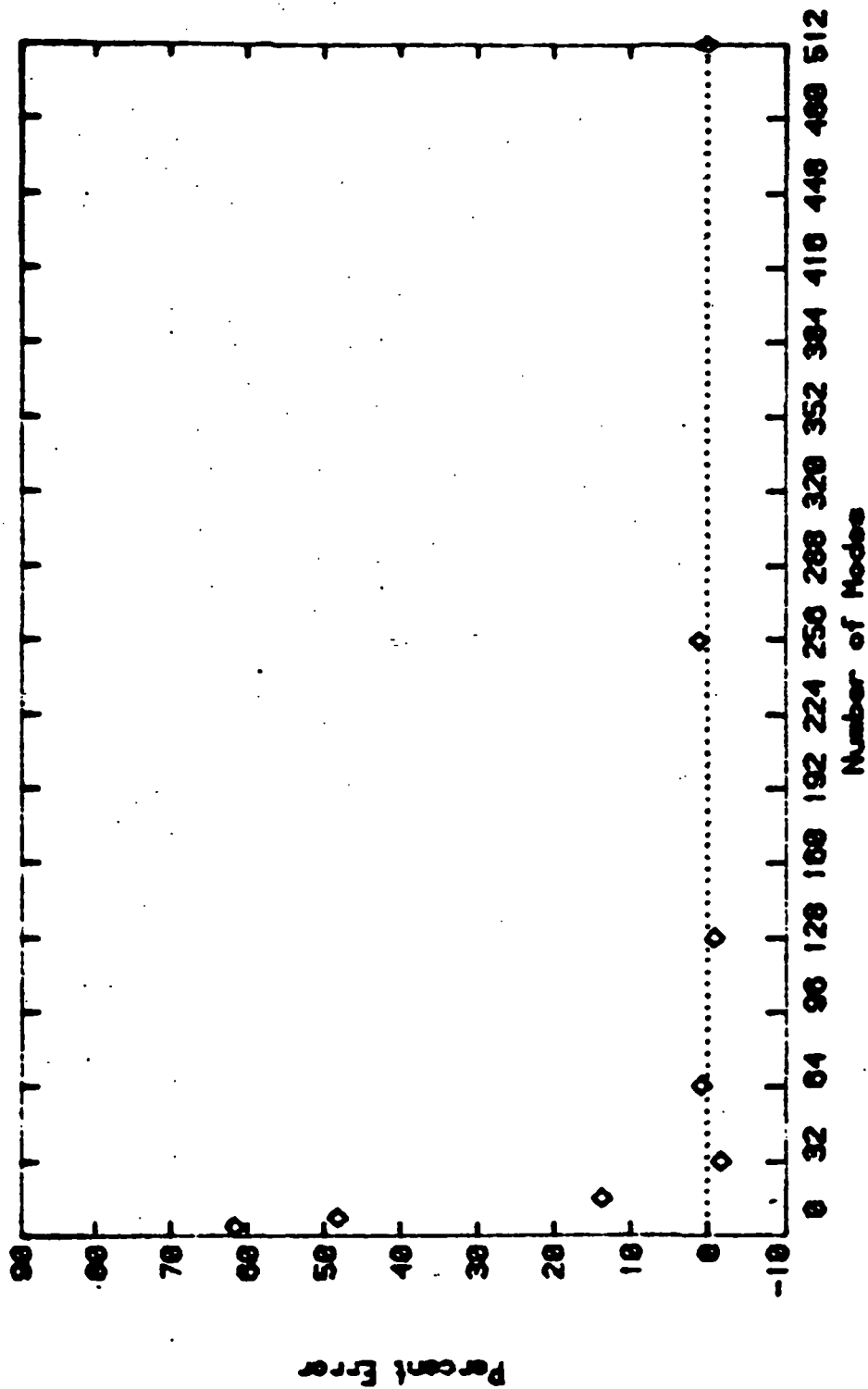


Figure 19. Illustration of converged accuracy for various number of terms with $a=0.25\lambda$, $b=0.247\lambda$, $\phi=0=0^\circ$ and $\sigma = \infty$ S.

VI. EXTENSION TO TWO-DIMENSIONAL PROBLEMS

The present analysis has been limited to fields having only one spatially varying component. When a second spatially varying component must be added, the difficulty in applying the contraction corrector scheme is increased. Each field component must have its own iteration equation as can be seen from equation (23). These equations are coupled, however, and this leads to new constraints that must be applied to the problem [12]. For iterative equations of the form

$$\begin{aligned} x_{n+1} &= f(x_n, y_n) \\ y_{n+1} &= g(x_n, y_n) \end{aligned} \tag{59}$$

in a space X , the sufficient but not necessary conditions for convergence are

$$\begin{aligned} \left| \frac{\partial f}{\partial x} \right| + \left| \frac{\partial f}{\partial y} \right| &< \rho \\ \left| \frac{\partial g}{\partial x} \right| + \left| \frac{\partial g}{\partial y} \right| &< \rho \end{aligned}$$

for all x, y in X where $\rho < 1$. As was observed in the one-dimensional case, the conditions for convergence revolve around the derivatives of the iterative equations. The determination of the partial derivative follows the form of equation (52) and may be written for $f(x_n, y_n)$ as

$$f_x = \frac{\partial f}{\partial x} = f_x(x_n, y_n) = \frac{f(x_n + \Delta x, y_n) - f(x_n, y_n)}{\Delta x} \quad (61)$$

where f_x indicates the partial derivative of $f(x, y)$ is taken. Again, it is seen that contraction theory allows the measure of the derivative to be calculated. The conditions to insure convergence must now be determined.

The conditions given in equation (60) are sufficient and not necessary and as such are fairly strong conditions. Thus if a stronger condition is applied, the stronger condition is also sufficient. Such conditions are

$$f_x = f_y = g_x = g_y = 0.0 \quad (62)$$

These conditions can not be met unless a new set of equations are formed using the contraction corrector method. The method for the one-dimensional case required the combining of x_n and x_{n+1} together to form a new iteration equation. The two-dimensional case requires the combining of

the x_n and x_{n+1} along with f_x , f_y , g_x , and g_y to meet the requirements of equation (60). A form of equation that conforms to the plan outlined above for x_{n+1} is

$$x_{n+1} = F(x_n, y_n) = \alpha x_n + (1 - \alpha) f(x_n, y_n) + \beta y_n - \beta g(x_n, y_n) \quad (63)$$

The first term of equation (63) is that of the one-dimensional case. The second term of equation (63) is seen to be equal to zero when y_n approaches the fixed-point y^* .

Similarly, the iterative equation for y_{n+1} is:

$$y_{n+1} = G(x_n, y_n) = [\gamma y_n + (1 - \gamma) g(x_n, y_n)] + [\partial x_n - \partial f(x_n, y_n)] \quad (64)$$

The complex constants α, β, γ , and ∂ are the contraction corrector terms that must be utilized to force equations (63) and (64) to meet the convergence requirements of equation (60).

The partial derivatives of equation (63) are set equal to zero and are found to be:

$$F_x(x_n, y_n) = \alpha + (1 - \alpha) f_x(x_n, y_n) - \beta g_x(x_n, y_n) = 0 \quad (65)$$

$$F_y(x_n, y_n) = (1 - \alpha) f_y(x_n, y_n) + \beta - \beta g_y(x_n, y_n) = 0 \quad (66)$$

From these equations, β may be solved in terms of α as:

$$\beta = \frac{\alpha + (1 - \alpha) f_x(x_n, y_n)}{g_x(x_n, y_n)} \quad \text{for } g_x(x_n, y_n) \neq 0 \quad (67)$$

which may be substituted into equation (65) to find:

$$\alpha = \frac{[g_y(x_n, y_n) - 1] \frac{f_x(x_n, y_n)}{g_y(x_n, y_n)} - f_y(x_n, y_n)}{\frac{[f_x(x_n, y_n) - 1] [g_x(x_n, y_n) - 1]}{g_x(x_n, y_n)} - f_y(x_n, y_n)} \quad (68)$$

If $g_x(x_n, y_n) = 0$, α is found from equation (65) as:

$$\alpha = \frac{f_x(x_n, y_n)}{f_x(x_n, y_n) - 1} \quad (69)$$

which is seen to be the same form as equation (34) in the one-dimensional case. This is expected since $F_x(x_n, y_n)$ is not affected by $g_x(x_n, y_n)$. β is found from equation (66) as:

$$\beta = \frac{(\alpha - 1) f_y}{1 - g_y} \quad \text{for } g_x(x_n, y_n) = 0 \quad (70)$$

The case $g_y(x_n, y_n) = 1$ is excluded for the problems of

interest as this would indicate multiple solutions. Multiple solutions are excluded from the problems presented herein since they are derived from Maxwell's equations and appropriate boundary conditions and, as such, uniqueness is guaranteed. The case that the denominator of equation (68) equals to zero requires closer examination. This case would yield an $\alpha \rightarrow \infty$. This implies that $x_n \approx 0$ as seen from equation (63) and this case is a trivial one for the problems of interest. Therefore, this special case is not considered. The α and β determined above then allow the iteration equation (63) to be solved for $x_{n+1} = F(x_n, y_n)$. With this corrected value of x_{n+1} , a similar set of contraction correctors may be calculated for y_n and y_{n+1} solved for. The contraction coefficients γ and δ are calculated as:

$$\delta = \frac{\gamma + (1 - \gamma) g_y(x_{n+1}, y_n)}{f_y(x_{n+1}, y_n)} \quad \text{for } f_y(x_{n+1}, y_n) \neq 0 \quad (71)$$

and

$$\gamma = \frac{[f_x(x_{n+1}, y_n) - 1] \frac{g_y(x_{n+1}, y_n)}{f_x(x_{n+1}, y_n)} - g_x(x_{n+1}, y_n)}{[g_y(x_{n+1}, y_n) - 1][f_y(x_{n+1}, y_n) - 1] - g_x(x_{n+1}, y_n) f_y(x_{n+1}, y_n)} \quad (72)$$

When $f_y(x_{n+1}, y_n) = 0$, arguments similar to those previous hold and the following correctors are obtained as:

$$\gamma = \frac{g_y(x_{n+1}, y_n)}{g_n(x_{n+1}, y_n) - 1} \quad (73)$$

$$\delta = \frac{(\gamma - 1) g_x(x_{n+1}, y_n)}{1 - f_x(x_{n+1}, y_n)} \quad (74)$$

The γ and δ are then used in equation (64) to find $y_{n+1} = G(x_{n+1}, y_n)$. The iterative process is then repeated until a suitable accuracy has been achieved. An example of this two-dimensional contraction corrector scheme is laid out in Table 4.

Even though the foregoing text and results of Table 4 have indicated that the contraction corrector method may be successfully applied to analytical two variable problems, it remains to be seen that the theory is directly extendable to numerical methods. Current results of the application of equations (63) and (64) with the correctors of equations (67) through (74) as applied to the one-dimensional problems of Sections IV and V agree with the previous data. However, the application of the contraction corrector scheme to a two-dimensional canonical problem has yielded poor results. The problem appears to be the numerical evaluation of the partial derivatives. Without the accurate de-

$$f(x, y) = x = 2x + 2y$$

$$g(x, y) = y = x^2 + 2y$$

$$F(x, y) = x = \alpha x + (1 - \alpha)f(x, y) + \beta y - \beta g(x, y)$$

$$G(x, y) = y = \gamma y + (1 - \gamma)g(x, y) + \delta x - \delta f(x, y)$$

n	x_n	y_n	$f(x_n, y_n)$	$g(x_n, y_n)$
0	1	1	4	3
1	4	3	14	22
2	14	22	72	240
3	-----diverges-----			

n	x_n	y_n	α	β	γ	δ	$F(x_n, y_n)$	$G(x_n, y_n)$
0	1	1	0.67	0.67	-	-	0.5	-
1	0.5	1	-	-	0	1	-	-0.25
2	0.5	-0.25	-	-	-	-	-	-
			$x^* = 0.5$		$y^* = -0.25$			

Table 4. Example of a two-variable contraction corrector method.

termination of f_x , f_y , g_x , and g_y , it is doubtful the contraction corrector method will be successful in arriving at a convergent solution. Another problem that is not readily apparent is the stringent conditions placed on the partial derivatives. Invoking such strong conditions as given in equation (60) may cause computational problems and eased or adjusted conditions may be necessary to reach a viable solution method. These problems are being investigated and useful results are expected in the near term [25].

The usefulness of the two-dimensional contraction corrector can not be underestimated. For instance, when a plane wave strikes a one-dimensional grating at an incidence angle that induces current along two axes, a cross-polarized scattered field will be generated. The two-dimensional nature of the problem must be addressed to obtain the valuable cross-polarized information. The solution for reflection of waves from actual mesh surfaces is also of interest and involves the use of the method detailed in this dissertation.

An illustration of an actual mesh surface is shown in Figure 20. The material is molybdenum wire coated with gold and woven in a double-knit fashion. Reflector surfaces of space-deployable antennas have surfaces of this nature and their reflection characteristics must be known to accurately predict their electrical performance. Figure

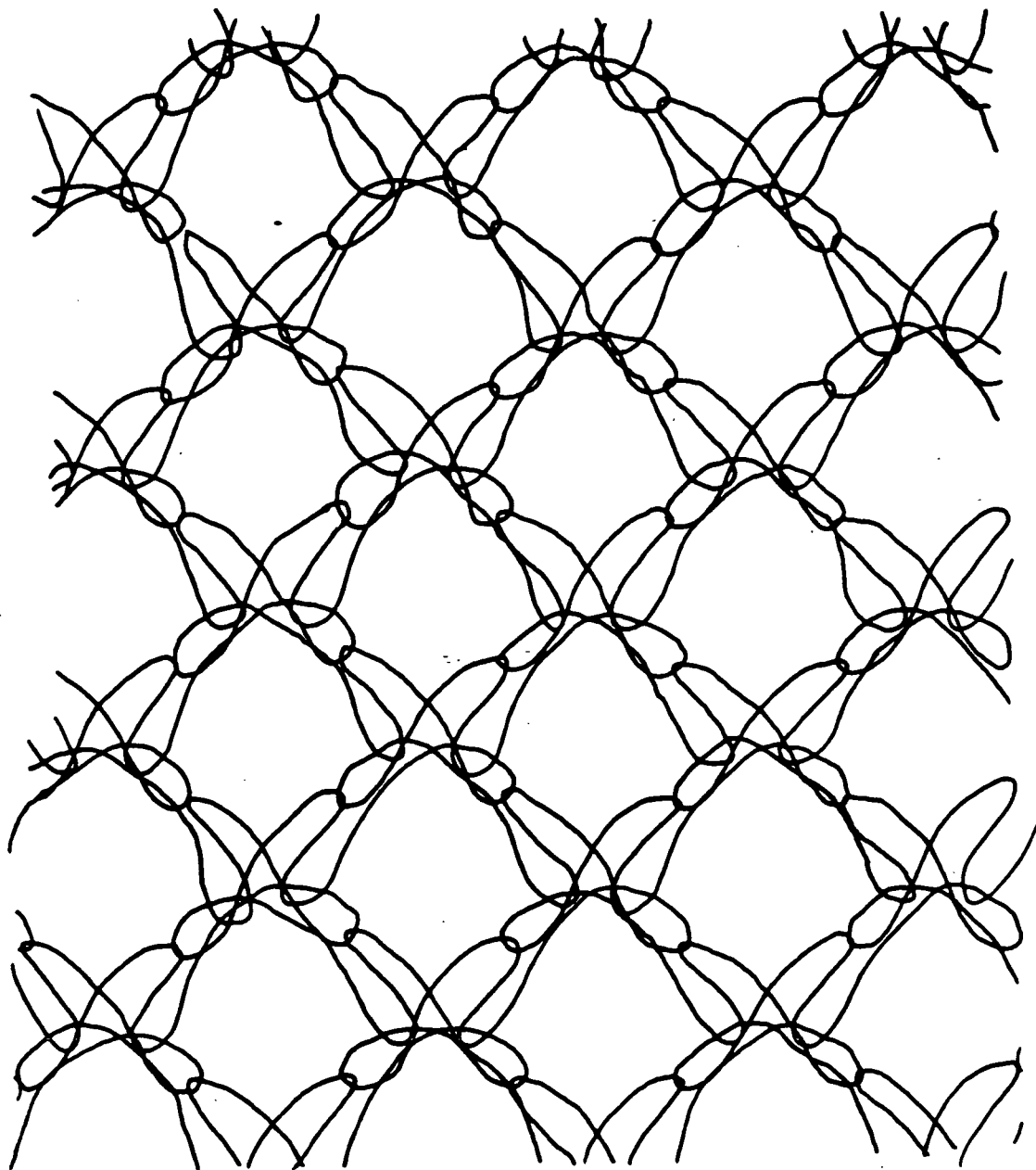


Figure 20. Actual mesh surface.

21 illustrates the periodic nature of the mesh surface. It can be seen from the outlined boxes that Floquet cells may be formed. This periodic nature may be capitalized on and used to formulate the mesh surface into a suitable problem for the contraction corrector scheme.

Figure 22 is the discrete representation of one single mesh path. The discretation of the mesh path is accomplished with twenty-eight, approximately equal length, straight segments. With these segments defined, it is possible to overlay a grid onto the segments to achieve a representation of the mesh surface. The equally spaced points on the grid represent the sampled points required for the Fourier Transform of the solution method. This typical grid representation of the mesh surface will allow the determination of the reflection characteristics of the surface. Other surface weaves and materials may be placed on similar grids and their reflection characteristics calculated. Figure 23 illustrates the application of the grid to the segmented single mesh path.

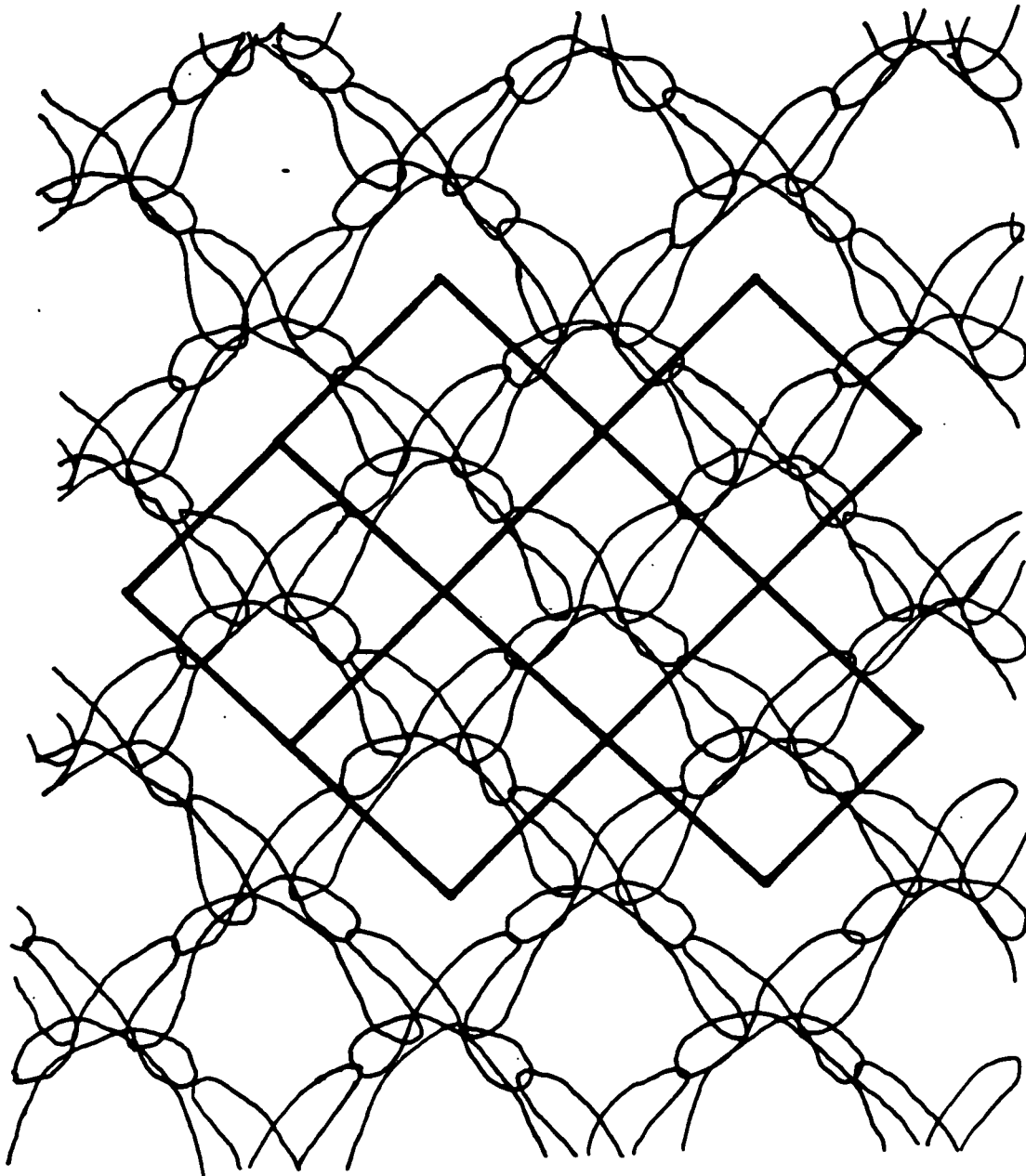


Figure 21. Floquet cells outlined on the actual mesh surface.

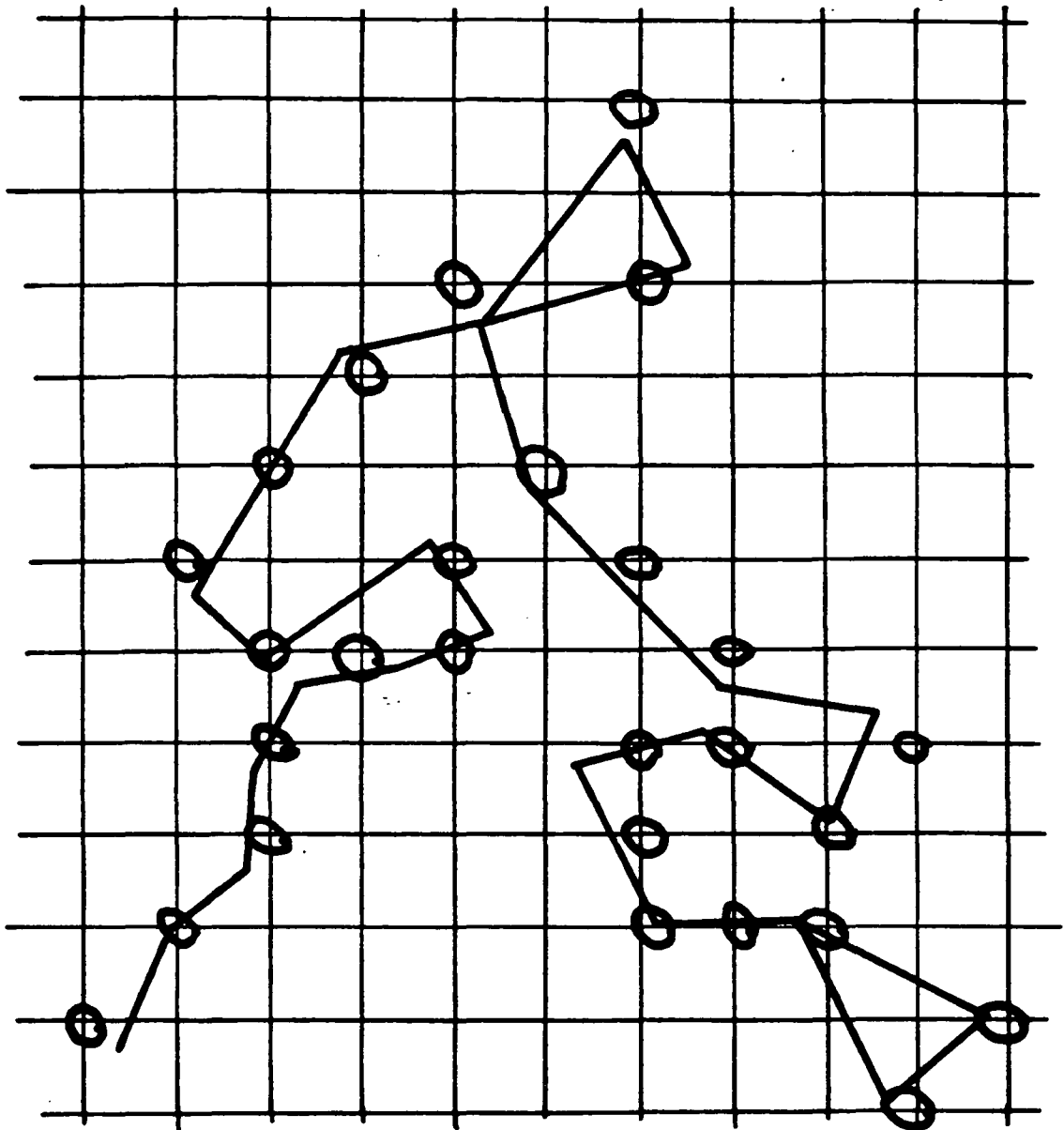


Figure 23. Grid representation of the segmented single mesh path.

VII. CONCLUSIONS

A new method called the contraction corrector method has been developed to insure the convergence of the one-dimensional spectral-iteration approach when solving electromagnetic scattering problems. The method was presented beginning with basic examples of the iterative method and progressing to detailed iterative operator theory. Computed data generated from the scheme was critiqued and compared to work previously presented and was found to agree well. The ability to predict the regions of solvability with the contraction corrector scheme was demonstrated. The method was then utilized to solve for the reflection coefficients from an infinite grating of thin wires and the results were compared to previously published data. The ideas of generalization to a two-dimensional problem were discussed. A solution technique for the two variable contraction corrector method was developed and numerical difficulties in applying the method were discussed. A sketch of an actual mesh surface was presented and the application of the spectral-iteration approach was detailed. A general reference list and an over-view of both the k-space problem formulation and the spectral-iteration approach were also included.

The material presented in this dissertation gives a solid foundation for future research, and indicates that a

suitable method for analyzing scattering from arbitrary mesh surfaces can be developed. The recommendations for future research should be directed toward understanding the shortcomings of the two-dimensional problem as detailed in Chapter VI. With the proper constraints placed on the two-dimensional problem and the correct evaluation of the partial derivatives, a suitable method of solution is deemed obtainable. Another alternative is the reformulation of the problem with another method of attack. Many numerical methods have yet to be applied to the problem and one may will be suited for the two-dimensional scattering problem.

REFERENCES

- [1] G.G. Macfarlane, "Surface impedance of an infinite parallel wire grid at oblique angles of incidence," IEE, No. 93, Part III A, pp. 1523-1527, 1946.
- [2] J.R. Wait, "Reflection at arbitrary incidence from a parallel wire grid," App. Sci. Res., Section B, vol. 4, pp. 393-400, 1954.
- [3] R.E. Collins, Field Theory of Guided Waves, McGraw-Hill, New York, 1960.
- [4] R.B. Kiebuntz and A. Ishimaru, "Scattering by a periodically apertured conducting screen," IRE Trans. Ant. and Prop., vol. AP-9, pp. 506-514, Nov. 1961.
- [5] N. Amitay and V. Galindo, "The analysis of circular waveguide phased arrays," BSTJ, pp. 1903-1932, Nov. 1968.
- [6] C.C. Chen, "Transmission through a conducting screen perforated periodically with apertures," IEEE MTT, vol. MTT-18, pp. 627-632, Sept. 1970.
- [7] S.W. Lee, "Scattering by dielectric-loaded screen," IEEE Trans. Ant. and Prop., vol. AP-19, pp. 656-665, Sept. 1971.
- [8] J.P. Montgomery, "Scattering by an infinite periodic array of thin conductors on a dielectric sheet," IEEE Trans. Ant. and Prop., vol. AP-23, No. 1, pp. 70-75, January 1975.
- [9] C.M. Tsao and R. Mittra, "A spectral-iteration approach for analyzing scattering from frequency selective surfaces," IEEE Trans. Ant. and Prop., vol. AP-30, No. 2, pp. 303-308, January 1982.
- [10] N.N. Bojarski, "K-space formulation of the electromagnetic scattering problem," Tech. Rep. AFAL-TR 71-75, March 1971.
- [11] J.C. Brand and J.F. Kauffman, "Analytic considerations for calculating the complex reflection characteristics of conducting mesh antenna surfaces," Int. Sci. Radio Union, Albuquerque, NM, May 1982.
- [12] S.D. Conte and C. DeBoor, Elementary Numerical Analysis, McGraw-Hill, New York, 1972, pp. 44 - 50.

- [13] R.F. Harrington, Time-Harmonic Electromagnetic Fields, McGraw-Hill, New York, 1961, pp. 27 - 34, 98 - 100.
- [14] V. Galindo and C.P. Wu, "Numerical solutions for an infinite phased array of rectangular waveguides with thick walls," IEEE Trans. Ant. and Prop., vol. AP-14, No. 2, pp. 149-158, March 1966.
- [15] A.B. Carlson, Communication Theory, McGraw-Hill, New York, 1975, pp. 56 - 58.
- [16] W.M. Patterson, Iterative Methods for the Solution of a Linear Operator Equation in Hilbert Space-A survey, Lect. Notes in Math, 394, Springer-Verlag, New York, 1974.
- [17] M. Altman, Contractors and Contractor Directions Theory and Application, Marcel Dekkar, New York, 1977.
- [18] I. Stakgold, Green's Functions and Boundary Value Problems, John Wiley, New York, 1979, pp. 243 -259.
- [19] A.V. Oppenheim and R.W. Schaffer, Digital Signal Processing, Prentice-Hall, Englewood Cliffs, NJ, 1975, Chapter 3.
- [20] M.I. Astrakan, "Averaged boundary conditions on the surface of a lattice with rectangular cells," Radio and Elec. Phys., No. 8, pp. 1239-1241, Aug. 1964.
- [21] J.C. Brand and J.F. Kauffman, "The application of the spectral-iteration approach to conducting mesh reflector surfaces," Int. Sci. Radio Union, Houston, TX, 1983.
- [22] E.C. Jordan and K.G. Balmain, Electromagnetic Waves and Radiating Systems, Prentice-Hall, Englewood Cliffs, NJ, 1968, pp. 144 - 150.
- [23] S.A. Schelkunoff, Electromagnetic Waves, Van Nostrand, New York, 1943, pp. 264.
- [24] J.P. Montgomery, "Analysis of frequency selective surfaces using the spectral-iteration approach," Int. Sci. Radio Union, Houston, TX, 1983.
- [25] C. Christodolou, J.C. Brand, and J.F. Kauffman, to be published.
- [26] R. Mittra, W. Ko, Y. Rahmat-Samii, "Transform approach to electromagnetic scattering," Proc. IEEE, vol. 67, No. 1, pp. 1486-1503, Nov. 1979.

- [27] M. Kontorovich, V. Petrun'Kin, N. Yesepkina, and M. Astrakhan, "The coefficient of reflection of a plane electromagnetic wave from a plane wire mesh," Radio Eng., vol. 7, pp. 222-231, 1962.
- [28] R.F. Harrington, Field Computation by Moment Methods, Reprinted by Roger F. Harrington, Cazenovia, New York, 1968, pp. 127 - 131.
- [29] R.F. Harrington, Time-Harmonic Electromagnetic Fields, McGraw-Hill, New York, 1961, pp. 223 - 225.
- [30] E.C. Jordan and K.G. Balmain, Electromagnetic Waves and Radiating Systems, Prentice-Hall, Englewood Cliffs, NJ, 1968, PP. 629 - 635.

The FORTRAN source code that follows will allow the user to solve for the electric field in the aperture of an infinite grating of thin wires as well as the reflection coefficient from the grating. The program is written in FORTRAN 4 and should run on most FORTRAN compilers with no modifications except the unit numbers on the read and write statements. The plot routine must be user supplied and the program modified accordingly. The input variables are specified in comments internal to the program. Comments are also included to help the user follow the flow of the program. Some of the variables are self explanatory and the others are listed below. A suitable DEL, the derivative increment, has been found to be (0.01,0.01) for most cases.

E(I)	Electric field in the aperture
JC(I)	Current density on the strip
G(I)	Transformed Green function
EUT(I)	Dummy E field variable
CREF	Complex reflection coefficient
HI	Incident H field
ED(I)	Incremented E field in the aperture
ALF(I)	Contraction corrector
CK?	Constants used in the iterative equation
K	Propagation constant
EOUT(I)	Output variable used for the external plot
Z	Internal impedance of the strip

<u>Lines</u>	<u>Program Flow</u>
170-400	Input data
410-520	Initialize parameters
530-610	Calculate incident \bar{E} and \bar{H} fields
620-640	Calculate thin wire impedance
650-720	Set up aperture/strip sample space
740-920	Calculate Floquet propagation constants and Green function transform
930-990	Initial aperture \bar{E}_a estimate
1020-1110	Calculate constants in iterative equation
1120-1130	Store untransformed \bar{E}_a
1140-1150	Take FFT of \bar{E}_a and $(\bar{E}_a + \text{DEL})$
1160-1200	Perform $G \bar{E}_a$
1210-1230	Take inverse FFT of $G \bar{E}_a$
1260-1290	Perform complement truncation $T_c(F[G \bar{E}_a])$
1300-1370	Perform FFT on $T_c(F[G \bar{E}_a])$
1380-1440	Perform $G^{-1} (F[T_c(F[G \bar{E}_a])])$
1450-1510	Calculate reflection coefficient
1520-1580	Perform inverse FFT on $G^{-1} (F[T_c(F[G \bar{E}_a])])$
1590-1610	Plot set up
1630-1670	Calculate contraction corrector
1680-1740	Apply contraction corrector if desired
1750-1780	Calculate finite conductivity effects
1790-1840	Perform FFT on first iterated E_a
1850	Test for five iterations, next iteration go to 1160
1880-1980	Output external plot and stop execution.

```

C
C***** FINAL.S **** D E R I V A T I V E   C O R R E C T *****
C Author      Jerry C. Brand
C DATE        August 12, 1963
C All rights reserved
C
C
C Dimension all arrays
  COMPLEX E(512),JC(512),G(512),EUT(512),DEL
  COMPLEX RI,CREF,HI
  COMPLEX ED(512),ALF(512),PRIME(512),U1(512),EDUT(512)
  COMPLEX J,CK1(512),CK2(512),CK(512),Z
  DIMENSION EOUT(512,10,2)
  REAL K,KZ
C A = Floquet cell dimension
C E = Strip size
  WRITE(6,*) ' INPUT FLOQUET CELL SIZE , STRIP SIZE'
  WRITE(6,*) ' NORMALIZED IN WAVELENGTHS'
  READ(5,*)A,B
C FREQ = Frequency in Hertz
  WRITE(6,*) ' INPUT FREQUENCY IN HERTZ'
  READ(5,*)FREQ
C MAX = FFT size = Number of samples per cell
C IW = log2(MAX) ; i.e. MAX=2**IW
C IP = 0 No plot; IP = 1 Plot;
C NOTE..... External plot routine required
C IAD = 0 No correction;
C IAD=1 Contraction corrector scheme applied
  WRITE(6,*) 'INPUT N, LOG2(N), PLOT OPTION, ADJUST OPTION'
  READ(5,*) MAX,IW,IP,IAD
C SIG = Conductance of strip
  WRITE(6,*) ' INPUT CONDUCTANCE OF STRIP IN SIEMANS'
  READ(5,*) SIG
C TH = Theta angle of incidence
C DEL = Complex increment used in derivative routine
C PH = Phi angle of Incidence
  WRITE(6,*) ' INPUT THETA ANGLE, DERIVATIVE DELTA, PHI ANGLE'
487 READ(5,*)TH,DEL,PH
  WRITE(6,16) DEL
16  FORMAT('-', ' DEL = ',2E10.4)
  IF(IAD.GE.1) WRITE(6,299)
299 FORMAT('-', ' A D J U S T M E N T   U S E D ')
C Initialize routine constants
  PI=3.141593
  TPI=PI*2.
  C=2.997956E+8
  UU=4.E-7*PI
  EP=8.854E-12
  ETA=SQRT(UU/EP)
  ITER=C
  J=(0.0,1.0)
  ALAMB=C/FREQ
  RD=180./PI
  DR=1./RD
C Calculate incident electric and magnetic field components
C for electric field parallel to wires, i.e. no cross-

```

ORIGINAL PAGE IS
OF POOR QUALITY

```

C polarization included
  IF(PH.LT.45.) EINC=1.0
  IF(PH.GE.45.) EINC=COS(TH*DR)
  IF(PH.LT.45.) STH=C.
  IF(PH.GT.45.) STH=TH
  HI=1./ETA*(COS(TH*DR)+J*SIN(TH*DR))
  IF(PH.LT.45.) HI=1./ETA*COS(TH*DR)
  Z=SQRT(TPI*FREQ*UU/2./SIG)*(1.0,1.0)/TPI/B
  WRITE(6,15) Z
15  FORMAT(' ', ' Z=(',E10.2,',',E10.2,',')')
C Calculate number of samples on strip and in aperture
  TAU=A-B
  N=IFIX(TAU/A*FLOAT(MAX))
  N1=N+1
  NM1=N-1
  MAX1=MAX+1
  WRITE(6,30) A,B,TAU,FREQ,TH,N,MAX
30  FORMAT(' ',3F10.5,E10.3,1F10.4,2I10)
  IF(N1.GT.MAX) GOTO 998
  K=TPI/ALAMB
  K2=K*K
  SK=K*SIN(TH*DR)*COS(PH*DR)
  SSK=K*SIN(TH*DR)*SIN(PH*DR)
  W=TPI*FREQ
  MAX1=MAX-1
C Calculate Green function transform
  DO 40 I=1,MAX
  IF(I.GT.MAX/2+1)GOTO 50
  U=TPI*(I-1)/A-SK
  GOTO 60
50  U=TPI*(I-MAX-1)/A-SK
60  U=U+U+SSK*SSK
  IF(U.GE.*2)GOTO 70
  G(I)=-J*SQRT(K2-U)
  GOTO 44
70  G(I)=-SQRT(U-K2)
44  G(I)=G(I)-SSK*SSK/G(I)
40  CONTINUE
C Initial E field estimate
  DO 320 I=1,N
  E(I)=(1.0,0.0)
320  ED(I)=E(I)+DEL
  DO 330 I=N1,MAX
  ED(I)=(0.0,0.0)
330  E(I)=(0.0,0.0)
C NOTE.... Iterative form used in this program is X = AX+E
C Calculate "B" portion of iterative equation
  DO 110 I=1,MAX
  110  CK1(I)=HI*J*W*LU
  CALL FFT(CK1,IW,MAX)
  DO 120 I=N1,MAX
  120  CK2(I)=HI*W*UU/J
  DO 140 I=1,N
  140  CK2(I)=(0.0,0.0)
  CALL FFT(CK2,IW,MAX)
  DO 130 I=1,MAX
  130  CK(I)=(CK1(I)+CK2(I))/G(I)

```

```

      DO 300 I=1,MAX
300 U1(I)=E(I)
      CALL FFT(ED,IW,MAX)
      CALL FFT(E,IW,MAX)
C Begin "AX" portion of iterative equation
C Perform (G+E)
      80 DO 100 I=1,MAX
          ED(I)=CONJG(ED(I)*E(I))
      100 E(I)=CCNJG(E(I)*G(I))
C Perform inverse transform of (G+E)
      CALL FFT(E,IW,MAX)
      CALL FFT(ED,IW,MAX)
      WRITE (3,199) ITER
      199 FORMAT(10X,I10)
C Perform truncation operation T(G+E)
      DO 150 I=1,N
          ED(I)=(0.0,0.0)
      150 E(I)=(0.0,0.0)
          DO 160 I=N1,MAX
              ED(I)=CONJG(ED(I))/MAX
              E(I)=CCNJG(E(I))/MAX
C Calculate current density on strip
      160 JC(I)=E(I)*J/W/UU-PI
C Perform inverse transform on T(G+E)
      CALL FFT(E,IW,MAX)
      CALL FFT(ED,IW,MAX)
C Perform T(G+E)/G and add constant "B"
      DO 170 I=1,MAX
          E(I)=E(I)/G(I)+CK(I)
          ED(I)=ED(I)/G(I)+CK(I)
          EDUT(I)=CONJG(ED(I))/MAX
          EUT(I)=CCNJG(E(I))/MAX
      170 CONTINUE
C Calculate reflection coefficient
      PI=J*SIN(STH*DR)/CCS(STH*LR)
      CREF=(E(1)/MAX+EINC()+J*SIN(STH*DR)*ABS(1.-ABS(E(1)/MAX+EINC())))
      CREF=CREF/(CCS(STH*DR)+J*SIN(STH*DR))
      REF=CABS(CREF)
      WRITE(6,453) REF,CREF
      453 FORMAT(6X," REF= ",F10.3,20X," CREF= ",F10.2,3X,F10.2)
C Perform inverse transformation to obtain first iterated
C electric field
      CALL FFT(EUT,IW,MAX)
      CALL FFT(EDUT,IW,MAX)
      DO 200 I=1,MAX
          EDUT(I)=CONJG(EDUT(I))
      200 EUT(I)=CONJG(EUT(I))
C Plot option
      IF(IP.LT.0) GOTO 180
      CALL JPLOT(EUT,MA),ITER,EDUT)
      180 ITER=ITER+1
C Call subroutine to calculate derivative of operator and
C contraction factor
      CALL DERIV(EUT,EDUT,"AX,PRIME,ALF,IAD,DEL,CON)
      WRITE(6,340) CON
      340 FORMAT(/,10X," CONTRACTION = ",F10.4)
C Perform correction on electric field; NOTE... If IAD=0

```

```

C no adjustment is used as ALF(1)=0.0
  DO 350 I=1,N
    EUT(I)=ALF(I)*U1(I)+(1.-ALF(I))*EUT(I)
    U1(I)=EUT(I)
  350 EDUT(I)=EUT(I)+DEL
  310 CONTINUE
C Calculate field on strip due to finite conductivity
  DO 210 I=N1,MAX
    EDUT(I)=-JC(I)+Z*B
  210 EUT(I)=-JC(I)+Z*B
C Perform transform of E field to begin next iteration
  CALL FFT(EUT,IW,MAX)
  CALL FFT(EDUT,IW,MAX)
  DO 220 I=1,MAX
    ED(I)=EDUT(I)
  220 E(I)=EUT(I)
    IF(ITER.GT.5) GOTO 240
    GOTO 80
  240 CONTINUE
    DO 777 I=1,MAX
      FINDEX=FLOAT(I-1)/FLOAT(MAX-1)*A
C Perform plot functions for external Plot routine
      WRITE(22,778) FINDEX,EOUT(I,1,1),EOUT(I,2,1),EOUT(I,3,1)
      +,EOUT(I,4,1),EOUT(I,5,1)
      WRITE(23,778) FINDEX,EOUT(I,1,2),EOUT(I,2,2),EOUT(I,3,2)
      +,EOUT(I,4,2),EOUT(I,5,2)
  778 FORMAT(6F8.2)
  777 CONTINUE
      WRITE(6,260)
  260 FORMAT('-',10X,' T I M E L L Y   E X I T ')
  998 WRITE(6,99)
  99  FORMAT('-', ' E R R O R   I N   N ')
9999 STCP
  END
  SUBROUTINE JRPLOT(A,INT,ITER,EOUT)
  COMPLEX A(1)
  DIMENSION AMP(512),EOUT(512,10,2),PHASE(512)
  N=ITER+1
  DO 80 I=1,INT
    AMP(I)=CABS(A(I))
    PHY=AIMAG(A(I))
    PHX=REAL(A(I))
    IF(ABS(PHX).LT.1.E-20) PHX=1.E-20
    PHASE(I)=57.295*ATAN2(PHY,PHX)
    EOUT(I,N,1)=AMP(I)
    EOUT(I,N,2)=PHASE(I)
  80 CONTINUE
  RETURN
  END
  SUBROUTINE DERIV(E,ED,MAX,PRIME,ALF,IAD,DEL,CON)
C This subroutine calculates the derivative and
C contraction factor of the operator
  COMPLEX E(MAX),ED(MAX),ALF(MAX),PRIME(MAX),DEL
  CON=C.C
  DO 10 I=1,MAX
    PRIME(I)=(ED(I)-E(I))/DEL
    CON=(CON+(CABS(PRIME(I)+DEL))*2

```

```

ALF(I)=PRIME(I)/(PRIME(I)-1.0)
10 IF(IAD.LT.1) ALF(I)=0.0
CON=SQRT(CON/FLGAT(MAX))/CABS(DEL)
RETURN
END

```

```

SUBROUTINE FFT(A,M,N)

```

C This is the FFT subroutine called from the main program

```

COMPLEX A(N),U,W,T
N=2**M
NV2=N/2
NM1=N-1
J=1
DO 7 I=1,NM1
IF(I.GE.J) GOTO 5
T=A(J)
A(J)=A(I)
A(I)=T
5 K=NV2
6 IF(K.GE.J) GOTO 7
J=J-K
K=K/2
GOTO 6
7 J=J+K
PI=3.141592653589793
DO 20 L=1,M
LE=2**L
LE1=LE/2
U=(1.0,0.0)
W=CMPLX(COS(PI/LE1),SIN(PI/LE1))
DO 20 J=1,LE1
DO 10 I=J,N,LE
IP=I+LE1
T=A(IP)*U
A(IP)=A(I)-T
10 A(I)=A(I)+T
20 U=U*W
RETURN
END

```

APPENDIX B

The general form of the basic iterative process is given as

$$\bar{E}_t^{(n+1)} = F^{-1} \left[\frac{\bar{G}}{G}^{-1} \cdot F \left\{ \frac{j\omega\mu_0}{2} \left[T_c \left(\bar{H}_{\text{tinc}} + \frac{2}{j\omega\mu_0} F^{-1} \left\{ \frac{\bar{G}}{G} \cdot F \left[T \left(\bar{E}_t^{(n)} \right) \right] \right\} - \bar{H}_{\text{tinc}} \right] \right\} \right] \right\} \right] \quad (\text{B1})$$

The linear operations indicated in equation (B1) may be easier to understand if a flow of the operations is presented. Figure B-1 illustrates the iterative process used in the computer program of Appendix A. The initial estimate of the electric field in the aperture is transformed and the transformed Green function is applied along with Floquet's theorem. The inverse transform is applied to this result to obtain the current density on the strip. The inverse of the previous steps is then performed to obtain the first iteration of the electric field in the aperture. That is, the current density is truncated over the aperture and transformed, the inverse transform Green function is then applied along with Floquet's theorem to obtain the iterated aperture electric field. This iterated electric field may then be truncated and the process repeated until a suitable solution and tolerable error is obtained.

Figure B-2 illustrates where the basic iterative pro-

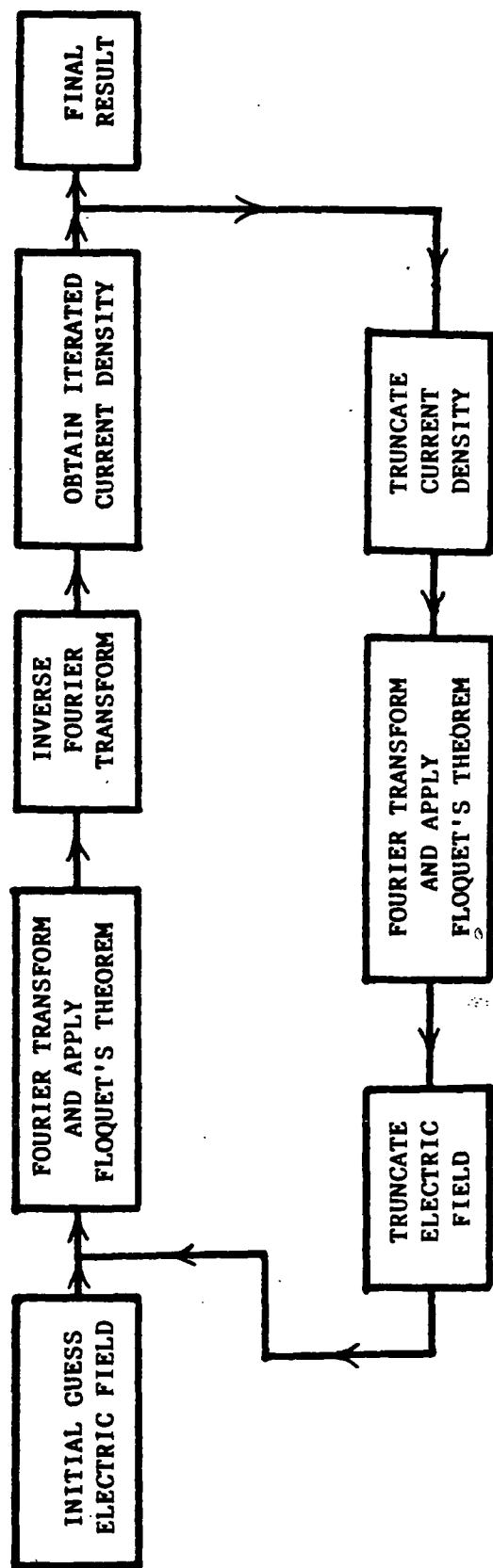


Figure B-1. The flow of the basic iterative process used in the text and in the computer program of Appendix A.

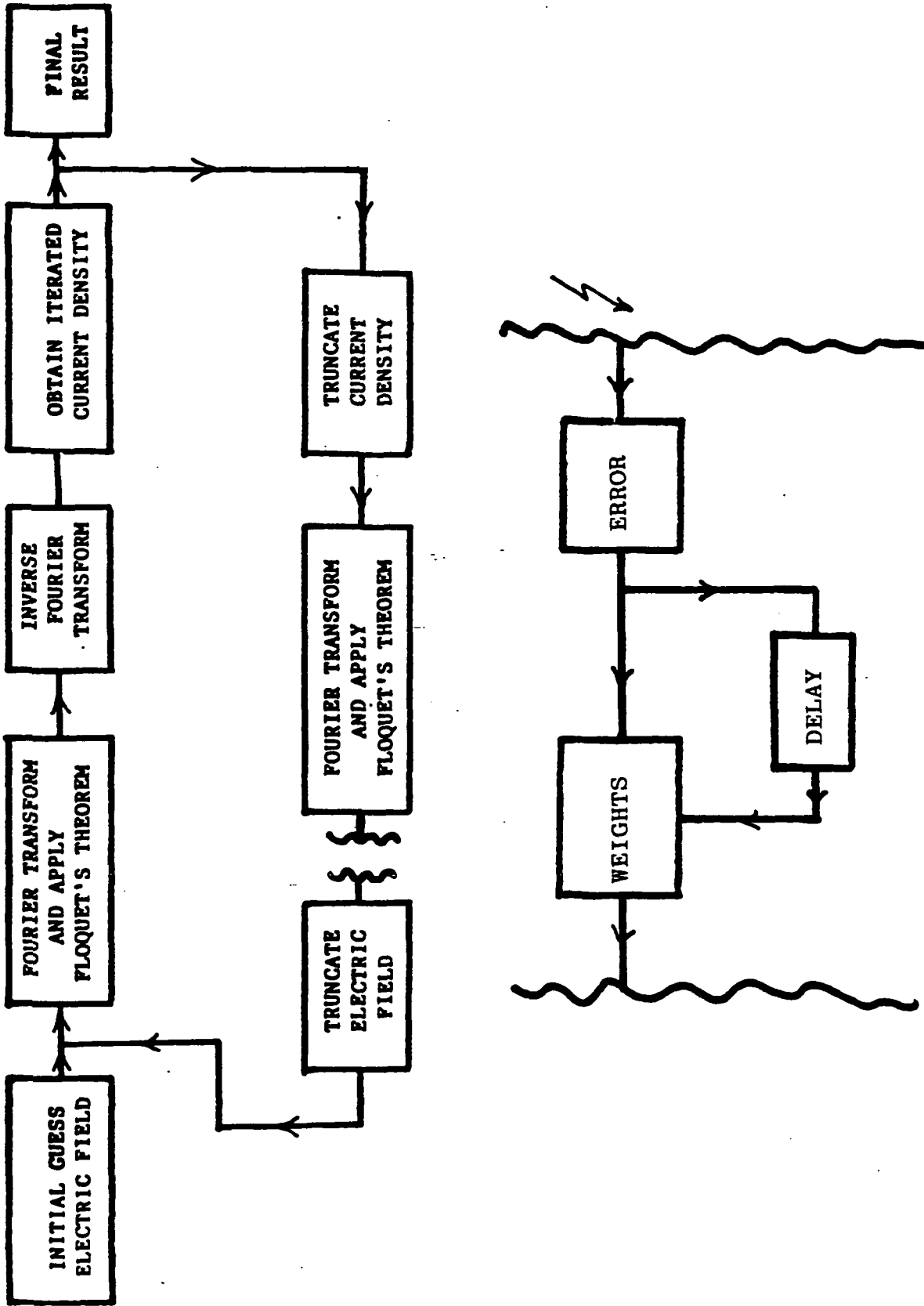


Figure B-2. The placing of the contraction corrector scheme in the basic iterative process.

cess may be interrupted to accommodate the contraction corrector scheme. This point is chosen since an iterated solution has been generated. With this iteration and any previous iterations a filtering process may be employed. The text pointed out the usefulness of the contraction corrector scheme since it guarantees a convergent solution. Thus, the iterative process can be viewed as a feedback process whereby the errors of processing can be eliminated and a useful solution of the problem obtained.

C-2

APPENDIX C

The optimum contraction corrector for the one-dimensional problem is shown to be equivalent to Newton's method. The proof is as follows:

$$f(x_n) = 0 \quad (C1)$$

$$G(x_n) = x_{n+1} = Rx_n + (1 - R) g(x_n) \quad (C2)$$

$$= \frac{g'}{g'-1} x_n + 1 - \frac{g'}{g'-1} g(x_n) \quad (C3)$$

$$= \frac{g'}{g'-1} x_n + \frac{g'-1-g'}{g'-1} g(x_n) \quad (C4)$$

$$= \frac{g'}{g'-1} x_n + \frac{-g(x_n)}{g'-1} \quad (C5)$$

$$= \frac{g'x_n - g(x_n)}{g'-1} \quad (C6)$$

$$= \frac{g'x_n - g(x_n) + x_n - x_n}{g'-1} \quad (C7)$$

$$= \frac{(g'-1) x_n}{(g'-1)} + \frac{x_n - g(x_n)}{g'-1} \quad (C8)$$

$$x_{n+1} = x_n - \frac{g(x_n) - x_n}{g'-1} = x_n - \frac{f(x_n)}{f'(x_n)} \quad (C9)$$

where $g' = \left. \frac{d}{dx} g(x) \right|_{x=x_n}$.